SRF

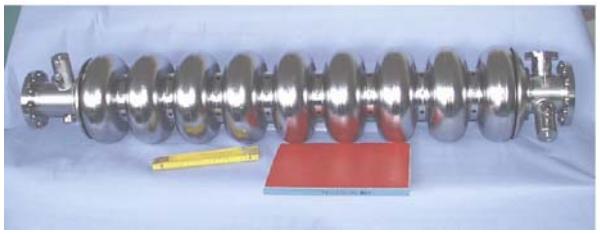

Deliverable 2.2.5.2:

Report on the Fabrication of New Cavity

P. Michelato, L. Monaco, N. Panzeri
INFN Milano, Lab. LASA,
Via Fratelli Cervi 201,
20090 Segrate (MI) - Italy

Abstract
New superconducting accelerator projects, like ILC, require a high accelerating field in order to reduce their footprint and cost. This report wants to be a contribution towards the realization of simpler and cheaper cavities. A cavity prototype has been built, equipped with a coaxial tuner and tested in horizontal cryostat. The results of the test gave indication for the design of a new end group proposal, fully compatible with the XFEL cavity and optimized for a future coaxial tuner use. Two end groups have been built for the mechanical characterization and for the verification of construction and welding procedures.

Acknowledgements

We acknowledge the support of the European Community-Research Infrastructure Activity under the FP6 “Structuring the European Research Area” programme (CARE, contract number RII3-CT-2003-506395)

Index

Introduction

In the last years a lot of R&D has been done on superconducting cavities aiming to develop a mature technology that could compete with the normal conducting one in the field of particle accelerators. The results were so good that in 2005 an International Panel selected this superconducting technology for the new linear collider, today called International Linear Collider (ILC).
The "secrets" that allowed to move in a short time span from an accelerating field of 5 MV/m to 25 MV/m or more are:

- an accurate check of the material purity and of its cleanliness;
- an accurate preparation of the parts to be assembled;
- a well defined sequence of treatments;
- adoption of clean handling procedures.

Nevertheless the ILC project requires more efficient cavities, with a design value of the accelerating field of 31.5 MV/m. This goal can be achieved only introducing some improvements in the manufacturing procedures and in the processing phase (electro polishing,…). Whatever the developments will be, they must be compatible with the overall cavity cost, possibly reducing it with the adoption of modifications that will lead to a "globally optimized" dressed cavity.
From this point of view our work wants to be a contribution towards the realization of simpler and cheaper cavities. The actual cavity design represents a starting point from which we based our R&D, mainly focused on the mechanical and manufacturing aspects.
Our approach was to develop a theoretical structural model based the existing geometry. This model was verified by means of cold tests performed on a modified dressed cavity in horizontal cryostat, and after that we developed new solutions, taking into account the following main aspects:

- compatibility with the actual tools and devices (lateral tuner, tuning tool, supporting devices, …);
- feasibility and economical aspects (discussed with one manufacturer);
- optimization towards the use of a coaxial tuner solution for the ILC project.

As the actual solution represents a starting point, a short review of the TTF cavity and of its production sequence is explained. After that we report some experimental results showing the effectiveness of our improvements (also with a non optimal solution), and at the end two different solutions (about the many developed) are presented, pointing out their pro and cons.

Existing solution

Description

The present cavity, when dressed (see Figure 1), is mainly composed of these parts:

- one end group, main coupler side, inclusive of one last half cell;
- one end group, without main coupler side, inclusive of one last half cell;
- internal dumb bells;
- an helium vessel with a lateral tuner.

As a consequence of the design choices this cavity requires a lot of steps for the welding of the end groups. Our work has been focalized on this item, starting to understand the welding procedure before trying any optimizations.

Figure 1: the TTF cavity ready to be installed in the cavity string.

End group welding procedure

The end group welding sequence and the preparation of reference surfaces are reported in Figure 2. The procedure is the same for both end groups: in the first step the NbRRR thin ring is welded, from the internal and external side, to the last half cell. Then the NbRG connecting ring is welded to the cell. In such a way two functions are accomplished: to stiffer the last half cell against the Lorentz Force detuning and to provide a good support for the end dishes. In the third phase the end dish is welded to the NbRG ring from the external side (the only one accessible). The last step is the weld n. 4 (from internal and external side) between the thin ring, the connecting ring and the cavity end pipe already prepared with flanges, HOM and pick-up. After the execution of welds 4A and 4B, the reference surfaces on the connecting ring are worked with high precision machines.
The final assembly is reported in Figure 3 .

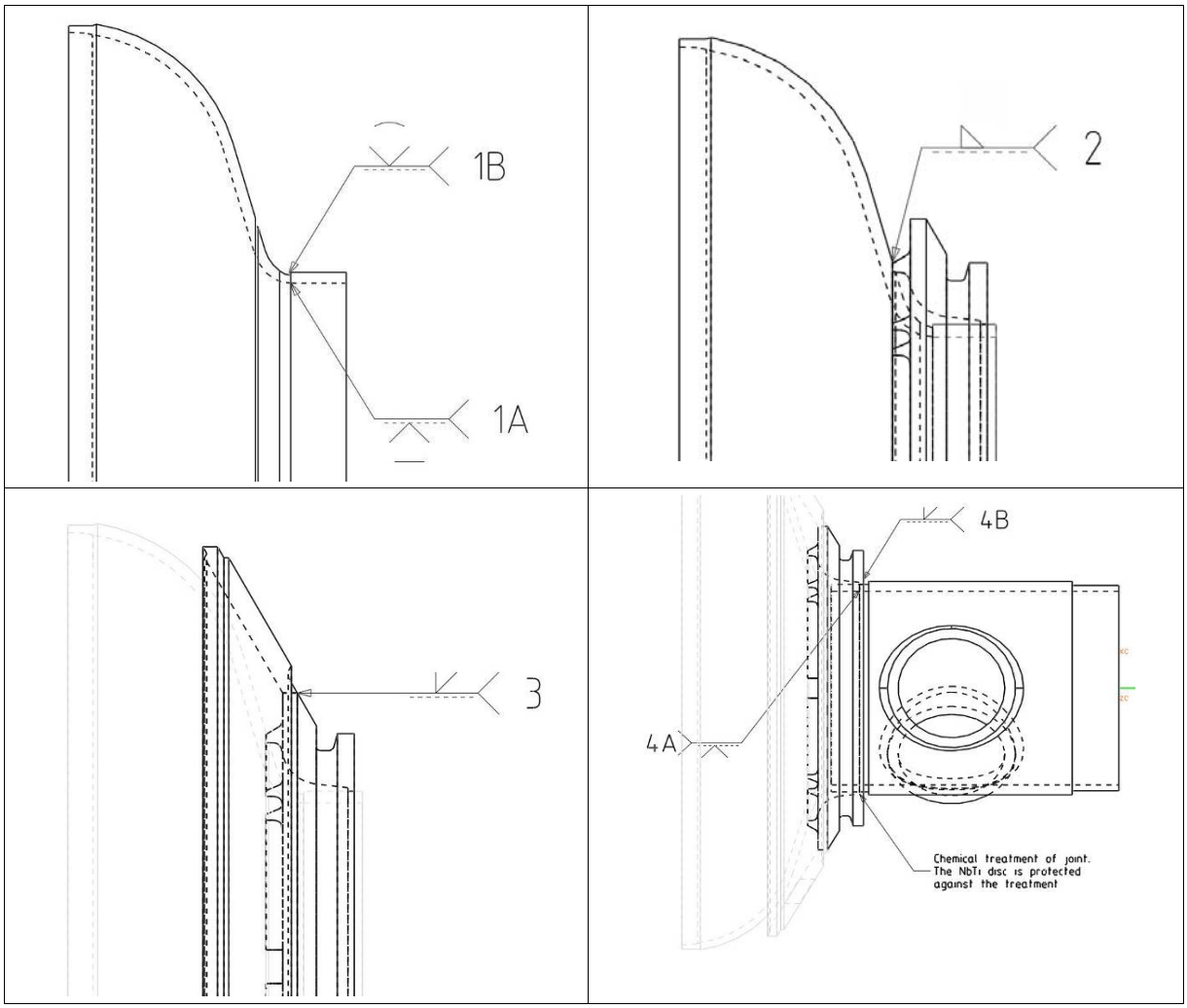

Figure 2: end group coupler side welding sequence. For sake of simplicity in the last weld sequence the HOM, pickup and flanges are not reported.

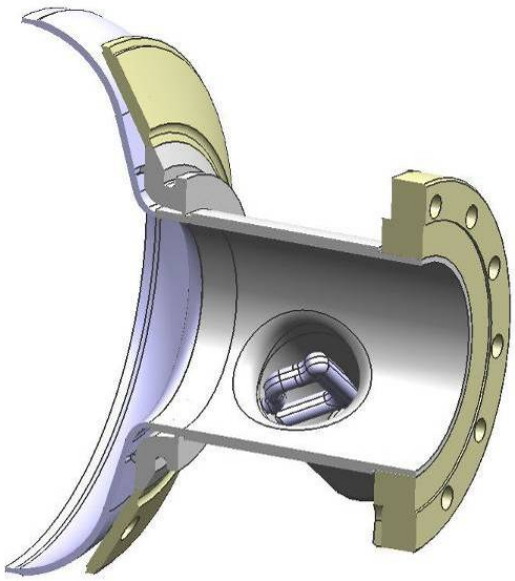

Figure 3: final assembly of the end group coupler side.

The first prototype

The design of the TESLA/XFEL/ILC cryomodule is driven by the request of a very high filling factor to reduce the accelerator length or to increase the effective accelerating field. The minimization of the inter-cavity distance is one of the critical point to reduce the accelerator footprint. As a consequence, the present ILC reference layout [1] assumes a coaxial tuner solution since the reduced total cell-to-cell space is incompatible with the current lateral tuner overall dimension.
The currently used helium tank is not compatible with a coaxial tuner solution; therefore we began our study on the cavity improvement developing a modified design of the end dishes and of their connection to the helium tank. The goal of these modifications was to have a design compatible with both the coaxial and lateral tuner.
The modifications introduced in the design were tested by means of several horizontal tests on a traditional cavity equipped with the modified helium tank and with the coaxial blade tuner. Although the geometry was not optimized due to the existing constraints, the results proved the effectiveness of the adopted solution and allowed to verify our theoretical model.

Modified Helium Tank

The helium tank is one of the components that assures the force transmission between the tuner and the cavity. Furthermore, if the coaxial tuner is used, it is also the part that allows the cavity elongation, differently from the actual design where the tuner displacements are allowed by the bellow, laterally positioned between one of the end dish and the helium tank.
Therefore, for the cold tests in horizontal cryostat, we decided to use an existing cavity and to modify the current helium tank design in order to satisfy the requirements imposed by the coaxial tuner solution. This allowed us to show the effectiveness of a different configuration implementing only minor modifications, preserving the cavity geometry and RF characteristics. After this preliminary step, we studied several end group design and choose the optimized one that is compatible both with the coaxial and lateral tuner solutions. In such a way all the procedures and tools developed up to now can be used and no experience is lost.
The modified helium tank is presented in Figure 4 and Figure 5. The differences with respect to the present solution are:

- the bellow allowing the tuner displacements is moved in the middle of the helium tank;
- the connection of the tank to the cavity end dishes does not require the bellow, that is now substituted by a rigid ring;
- the helium tank is equipped with two rings for the tuner assembly.
-

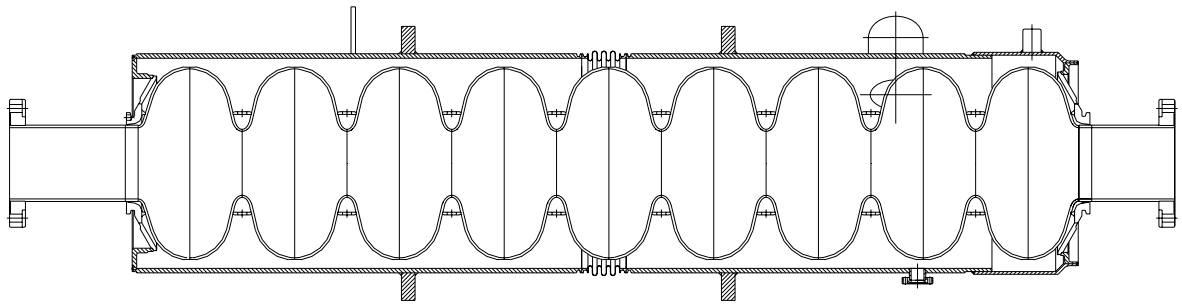

Figure 4: drawing of the cross section for the cavity assembly with the modified He tank.

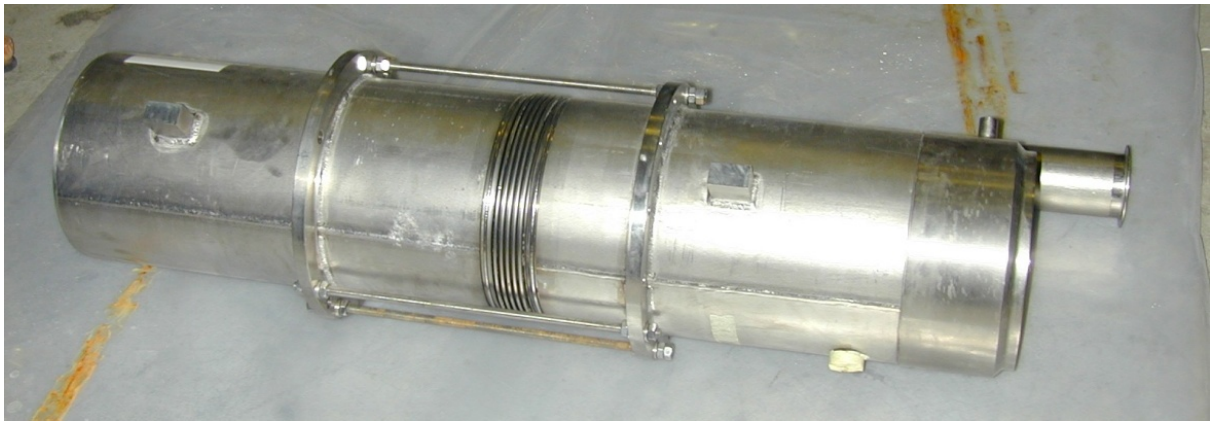

Figure 5: the modified He tank. The safety rods, installed between the welded rings, are temporally placed to save the bellow from unwanted deformations.

An essential role for what concerns the overall longitudinal stiffness of the assembly is played by the two cones that connect the vessel to the cavity, usually named as end dishes. For the modified Blade Tuner He tank, the end dishes have been adapted from the original TTF design without any optimization. The evaluation of their stiffness has been done by means of the axisymmetric 2D finite element model reported in Figure 6a.

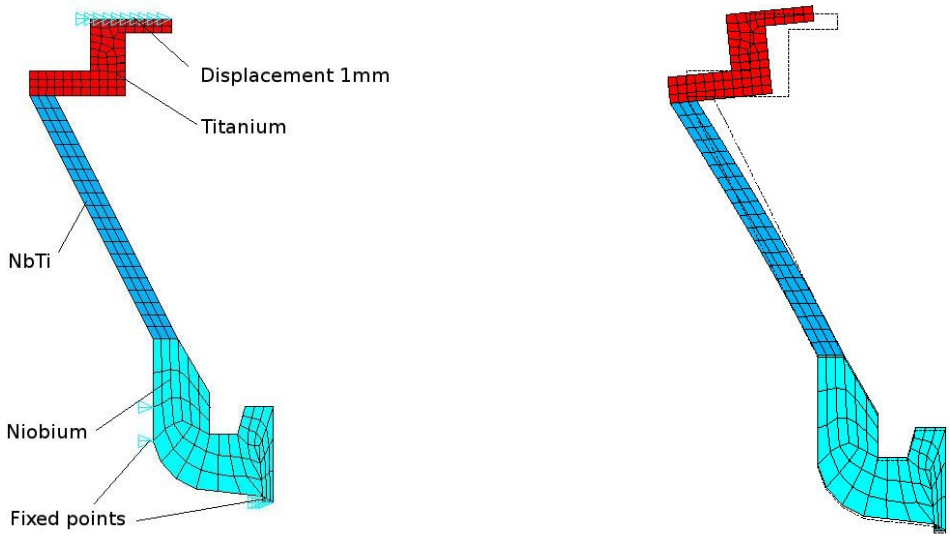

a: FE model b: deformation

Figure 6: end disc coupler side.

By imposing a displacement of 1 mm at the model upper edge, the structure reacts with a force that corresponds to an equivalent stiffness k_W^C of 24.8 kN/mm. The displacement obtained is shown in Figure 6b. A similar analysis carried out on the end dish at the opposite side (tuner side) that has a different design, reveled a higher stiffness value k_W^T of 32.2 kN/mm. These two results allowed to estimate the overall longitudinal stiffness k_W of the whole assembly composed by the series of both end dishes. Therefore:

$$k_W = \frac{k_W^C \cdot k_W^T}{k_W^C + k_W^T} = 14\,kN/mm\,.$$

The behavior of the new design was then evaluated inserting k_W and the stiffness of the other elements in the spring model shown in Figure 7. In particular we were interested to evaluate the effectiveness of the modified helium tank design to transfer the tuner displacements and forces to the cavity. The obtained results are reported in tables 1 to 4.

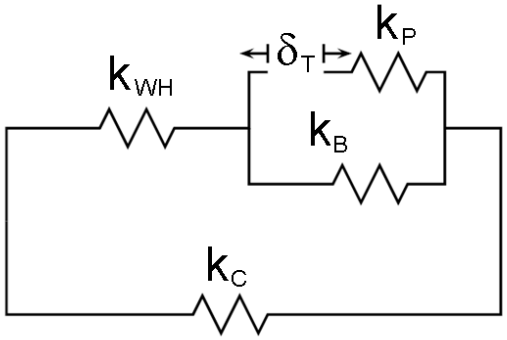

Figure 7: spring model of the dressed cavity: tuner (T), piezo (P), bellow (B), end dish + tank (WH), cavity (C).

Part	Force for a δ_t = 1 mm (kN)
Helium tank / End dishes	-2.435
Blade Tuner	-2.623
Cavity	2.435
Piezo actuators (total force)	-2.623
Tuner bellow	0.188

Table 1: axial forces for a tuner displacement of 1 mm. Tensile forces are positive.

Part	Displacement for a δ_t = 1 mm (mm)
Helium tank / End dishes	-0.182
Blade Tuner	1
Cavity	0.806
Piezo actuators	-0.013
Tuner bellow	0.988

Table 2: axial displacements for a tuner displacement of 1 mm. Elongations are positive.

Part	Force for a δ_p = 1 μm (N)
Helium tank / End dishes	-2.229
Blade Tuner	-2.401
Cavity	2.229
Piezo actuators (total force)	-2.401
Tuner bellow	0.172

Table 3: axial forces for a piezo actuators displacement of 1 μm. Tensile forces are positive.

Part	Displacement for a δ_p = 1 μm (μm)
Helium tank / End dishes	-0.167
Blade Tuner	-0.096
Cavity	0.737
Piezo actuators	1
Tuner bellow	0.904

Table 4: Axial displacements for a piezo actuators displacement of 1 μm. Elongations are positive.

Test results

The modified helium tank with the blade tuner has been tested at room and at cryogenic temperature to verify the modified design. The cavity used is the Z86 that exhibits a maximum accelerating field of 24.5 MV/m (Table 5)
At the time of tests the tuner design was not already finalized, therefore we used a special prototype made of stainless steel and Inconel 718.

Cavity	Z86	
Manufacturer	Zanon, I	
Arrival at DESY	22/04/05	
Weight	26.55	kg
BCP sessions	1	
BCP out	< 10	μm
EP sessions	3	
Material removed by EP	242.1	μm
Heat treatment	800° , 2h	
	127° , 48h	
RRR	296	
E_{acc} , V1	24.5	MV/m
Q_0 , V1	1.8 E10	
Field Flatness , last tuning	97	%
Frequency , last tuning	1297.333	MHz

Table 5: summary of Z86 cavity treatments and performances.

The experiments were performed at Desy (CHECHIA) and at Bessy (HoBiCat). Here we report the main results obtained in Bessy, where the helium tank, cavity and tuner have been extensively tested.
The full Blade Tuner frequency range was measured using the cavity closed in PLL loop to track cavity frequency displacement. It took 205000 motor steps (Phytron motor + Phytron gearbox), corresponding to 10 complete turns of the CuBe screw, to cover the desired tuning range of about 520 kHz, where the frequency range was kept to this value to have a direct comparison with the former test inside CHECHIA. The measure has been repeated three times, although the last time we stopped at one half of the trip backward (100000 steps) to perform the short range measurements. Figure 8 shows a comparison between the experimental results obtained at BESSY and at DESY and the expected ones based on our spring model. The shift between the two experimental curves is a consequence of the different piezo preload applied in the two tests.

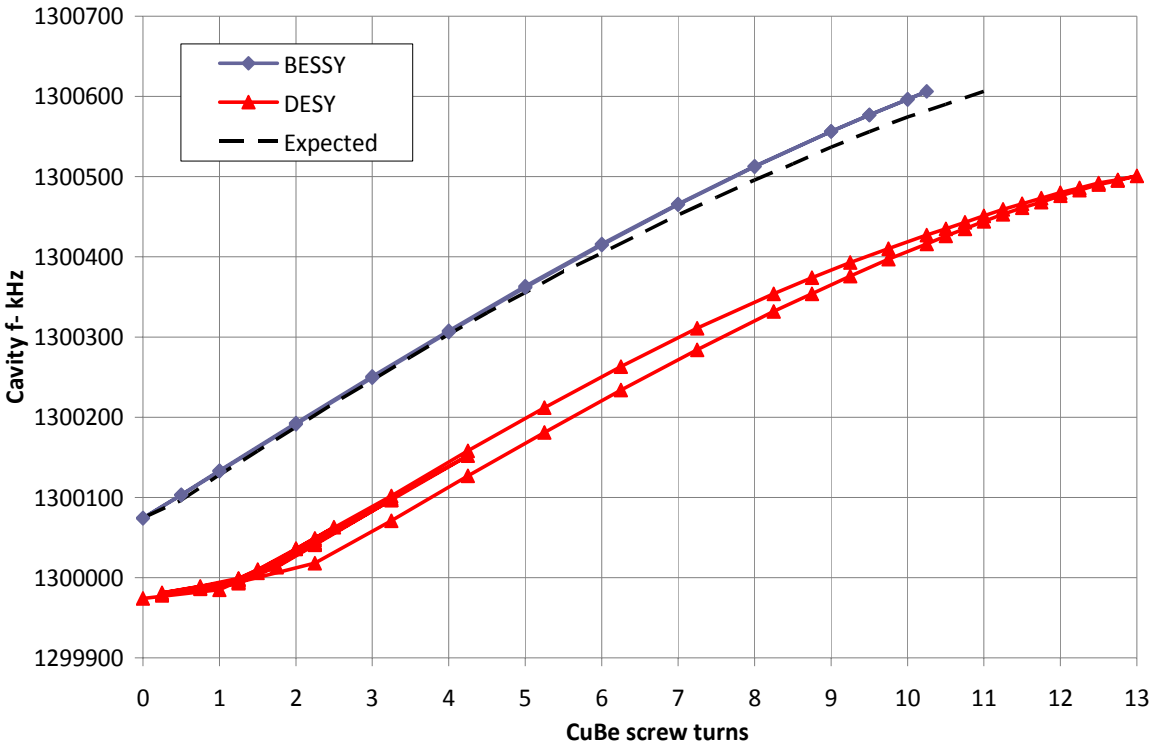

Figure 8: comparison between the two graphs taken during the tuning range tests inside CHECHIA and HoBiCaT. The reduction of the curve hysteresis is evident.

Conclusion on the first prototype results

The cold test on the modified dressed cavity, equipped with the coaxial blade tuner, were successful, proving that our model predicted very well the mechanical behavior of the main parts and that the modified helium tank does not complicate the preparation of the experimental test. Moreover these experiments allowed us to identify some aspects that we would to optimize in the following described proposals.

Proposals for future optimized solutions

As seen in the previous section the configuration of the cavity equipped with the blade tuner, and tested in Chechia and in HoByCat, has been greatly influenced by the existing components. The end groups geometry was unmodified and two adapting rings were used to assembly the cavity into the new helium tank. Moreover, the helium tank geometry was maintained as much as possible similar to the existing one, with the modifications confined to the introduction of the central bellow and to the repositioning of the pad [2] in order to have a better weight distribution.
For these reasons the configuration tested is not the optimum one. A better behavior and less expensive solution is expected with the introduction of some simplifications in the end group region. Here we describe two different proposal: the first one maintains the reference surfaces used in TTF and XFEL projects, therefore there should not be the necessity to change the tools for cavity tuning and positioning. The second solution is, in our opinion, as simple as possible, with the reference surfaces moved as in the 3.9 GHz cavity of the XFEL project [3]. This solution should also be the cheapest one, but, as it will be shown, it suffers high stresses in the area of connection between the cavity, the end dish and the end pipe.
Both the solutions have in common the removal of the end cell stiffening profile. This modification allows to change the welding procedures with a not negligible reduction of the numbers of electron beam weld and of their costs. Conversely, from our computations this should lead to an increase of the Lorentz Force Detuning (LFD) of about only 6%.
Moreover, minor deformations on the end cells are expected during the cavity welding procedure: a simplification of the tuning procedure for this part is expected.

The influence of the end cells stiffening

The end cells stiffening influence the Lorentz force detuning. According to our evaluation, the effect of the stiffening ring to the end cells is marginal (+6% increase), and could be avoided allowing a great simplification in the fabrication stages. This is consistent with our previous work on the SNS cavities, where we did not include any end-cell stiffening.

Numerical analyses

The Lorentz force calculations have been performed for a fully constrained cavity length, i.e. the cavity length does not change. Only the “intrinsic” factor due to the change in shape is thus computed. If the cavity is allowed to change its length, the additional term due to the longitudinal frequency sensitivity (approx. 350 Hz/μm) needs to be included in the evaluation.
The geometry and loads are taken from a 2D RF (SUPERFISH) computation, for a nominal TTF cavity, under field flatness condition. Nodes for the 2D FEA model are extracted from the geometry and the pressure load at each node is computed from the RF fields magnitude.
The geometry and load case are then fed into a mechanical (ANSYS) FEA computation, where nodal displacements are evaluated. From the nodal displacements the frequency offset is evaluated, through a perturbation technique (Slater theorem).
In the case of a finite stiffness provided to the constraint holding the cavity length, characterized by a stiffness K_{ext} (in N/mm), with a frequency sensitivity of 350 kHz/mm and a cavity spring longitudinal constant of 3500 N/mm, we have:

$$K_L^{real} = K_L^{stiff} - \frac{11500}{K_{ext} + 3500}\left[\text{Hz/(MV/m)}^2\right]$$

thus the LFD K_L factor "jumps" to approximately -3.7 Hz/(MV/m)^2 in the case of a completely free cavity, as it is graphically shown in the following figure.
As we can see from the following figure, the influence of any mechanical element that impacts strongly the stiffness provided against the cavity length variation results in a drastic increase in the LFD factor.

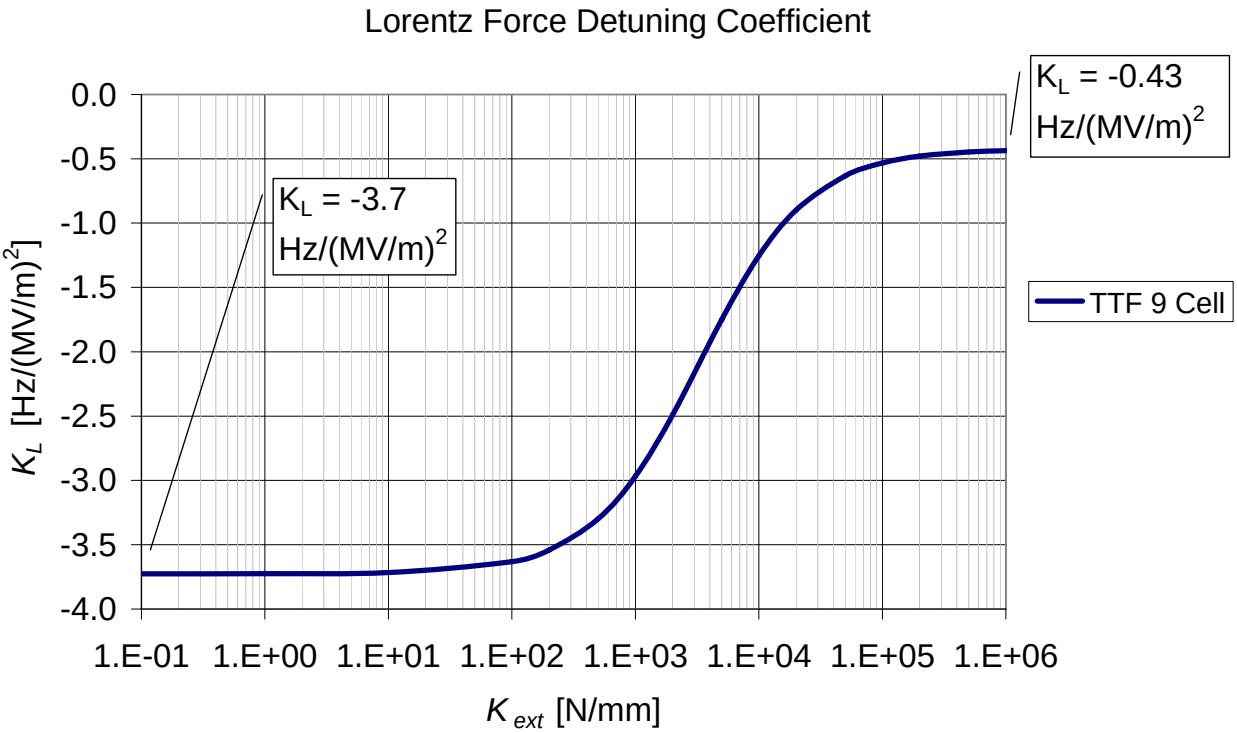

Figure 9: K_L factor behavior vs. the stiffness (K_{ext}) of the mechanical environment constraining the cavity length.

Slater Calculation without stiffeners at end rings

The deformation of the cavity due to the Lorentz forces has been computed with an axisymmetric model. The points ad the cavity extremities have been constrained in X and Y direction. Also the rotation ROTZ has been constrained. Using the Slater's formula the Lorentz detuning coefficient is equal to K_L=-0.451418 Hz/(MV/m)^2

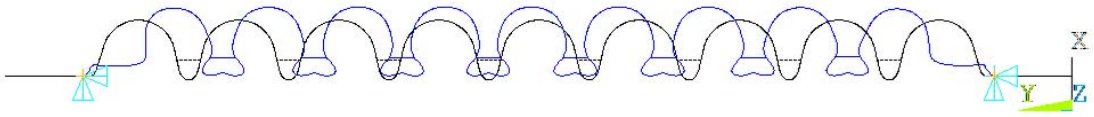

Slater Calculation with stiffeners at end rings

In this case the position corresponding to the stiffening ring has been constrained. The last half cells deforms less and the Lorentz detuning coefficient is equal to K_L=-0.424359 Hz/(MV/m)^2

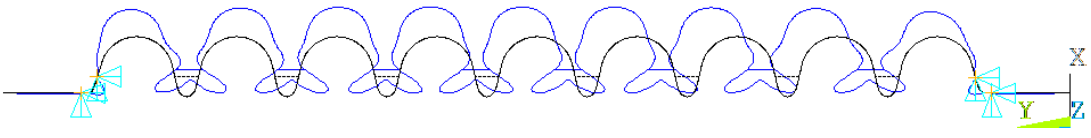

Comment

The difference in the K_L due to the change in the transverse shape is very small (increase of 6% due to the unstiffened end cell contribution). The effect of the finite stiffness constraint under real conditions is surely higher, due to the large sensitivity of the cavity frequency to a variation of the cavity length (coefficient of approx. 350 Hz/μm).

First solution (internal number 2.3.2)

Geometry of the modified parts (2.3.2)

The proposed 2.3.2 end groups are different from the TTF solution, but they maintain the reference surfaces on the Nb ring. In such a way the already developed tools and procedures (tuning, alignment in the clean room, etc…) remain unchanged. Furthermore in order to reduce the number of welds and manufacturing operations, the whole ring is realized in Nb RRR. The reduced dimensions respect to the actual solution makes this choice comparable with the previous one from the economical point of view.
The technical drawings of the main parts involved in this proposal are reported in appendix A. It can be noted that the end dish interface to the helium tank is the same of that actually used. As a consequence, the simplification introduced is compatible with the use of the lateral tuner and of all the devices used so far for the cavity handling.

End group preparation (2.3.2)

The foreseen welding steps are reported in figure 10. Only two loading in the EB welding machine are required: in the first one the end dish is welded to the NbRRR ring, while in the second one the end cell and the pipe are assembled to the ring.

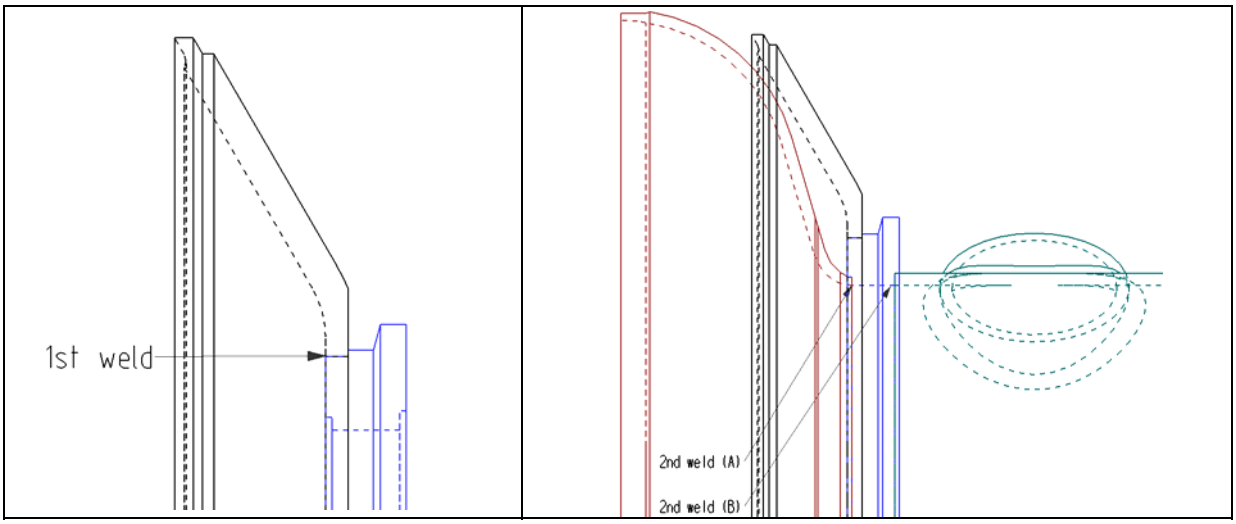

Figure 10: welding sequence.

Helium tank and its interface to the cavity (2.3.2)

The proposed solution is compatible to the TTF/XFEL cavity and to the Saclay tuner. Therefore, the helium tank to be used will be the standard one. In case of coaxial tuner choice, a further optimization can be obtained manufacturing the end dishes with a larger outer diameter (see Figure 11): in this case the helium tank must be modified as, for instance, proposed in our second solution.

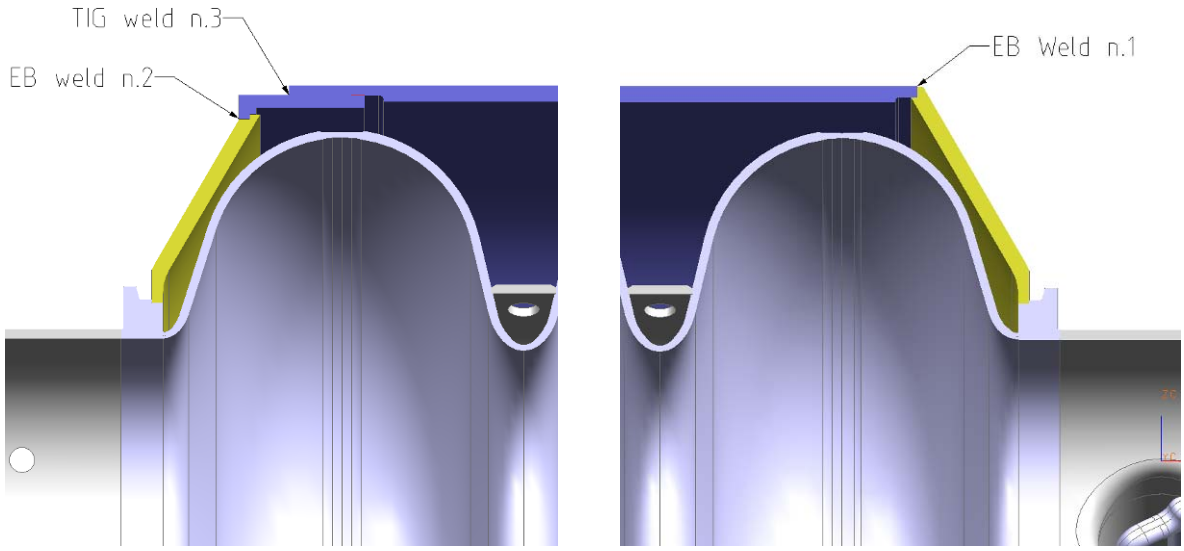

Figure 11: possible solution for the proposal 2.3.2 integrated in a helium tank equipped with the coaxial tuner.

Mechanical analysis of end group coupler side (2.3.2)

In this section the stress analysis of the end group (coupler side) is presented. Since the other end group has a similar shape, the same conclusions can be applied. The deformations and stresses of the end dish, in different load conditions, are evaluated by means of a Finite Element linear analysis. The numerical model considers all the structural parts between the cavity and the interface to the helium tank, that are the NbRRR ring, the end dish and the adapting ring. In such a way the obtained results can be directly compared with the second proposal (2.5.1) described later.

The material properties at room temperature are reported in table 6, while the axisymmetric mesh is reported in figure 13(a).

Before showing and discussing the analysis results it is important to point out the peculiarity of the welded area between the NbRRR ring and the NbTi dish. From the material properties it is evident the significant difference of the yield limits: 40 MPa for the NbRRR ring and 480 MPa for the end dish. In the welding zone the yield limit is unknown: it depends on many parameters and no data are available in literature. The FE model does not consider this aspect: the two parts are modelled without the weld mixed zone, meaning that a very small stress concentration area happens at the interface between the ring and the end dish. The extension of the plastic strains has been evaluated by means of a second analysis that takes into account the material non linearity of the heat treated at 800°C NbRRR.

Evaluation of the end group stiffness (2.3.2)

In order to evaluate the axial stiffness of the proposed end group an analysis has been performed applying a force of 8667 N at the top of the adapting ring. This force corresponds to the maximum reaction that the cavity transmits to the coaxial tuner when driven at the end of the tuning range (14 CuBe screw turns in figure 12, corresponding to +600 kHz) [4]. In this analysis the materials have been considered indefinitely elastic and the obtained maximum displacement is equal to 0.283 mm. The axial stiffness of the end dish at the coupler side is equal to 8667/0.283 = 30.6 kN/mm. The plot of the displacements and of the von Mises stresses are reported in figure 13(b) and (c).

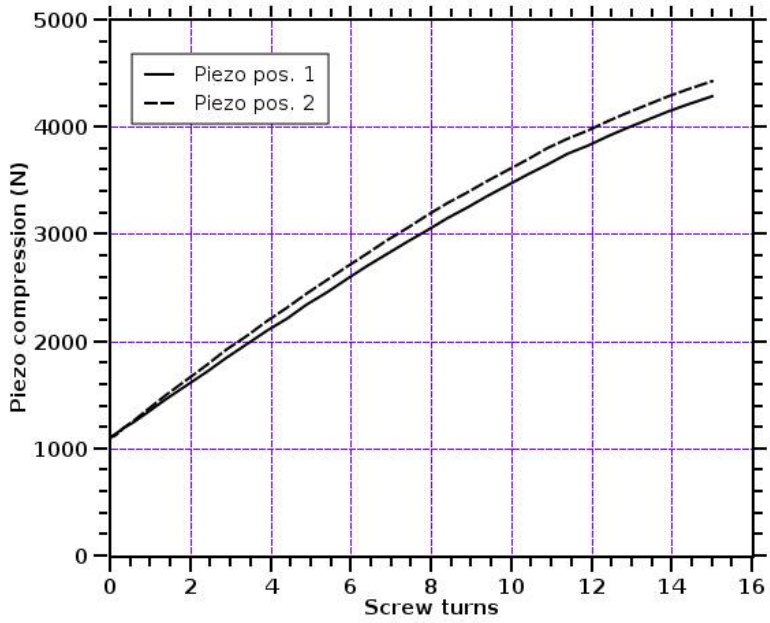

Figure 12: compression forces on the piezo elements (traction on the cavity) in the whole tuning range.

Material / Item	Ex (MPa)	ν	f_y (MPa)	E_{tang} (MPa)
Nb RRR / ring	102700	0.38	40*	2080
NbTi / end disc	62055	0.38	480	---
Ti Gr2 / adapting ring	105000	0.38	275	---

Table 6: material properties.

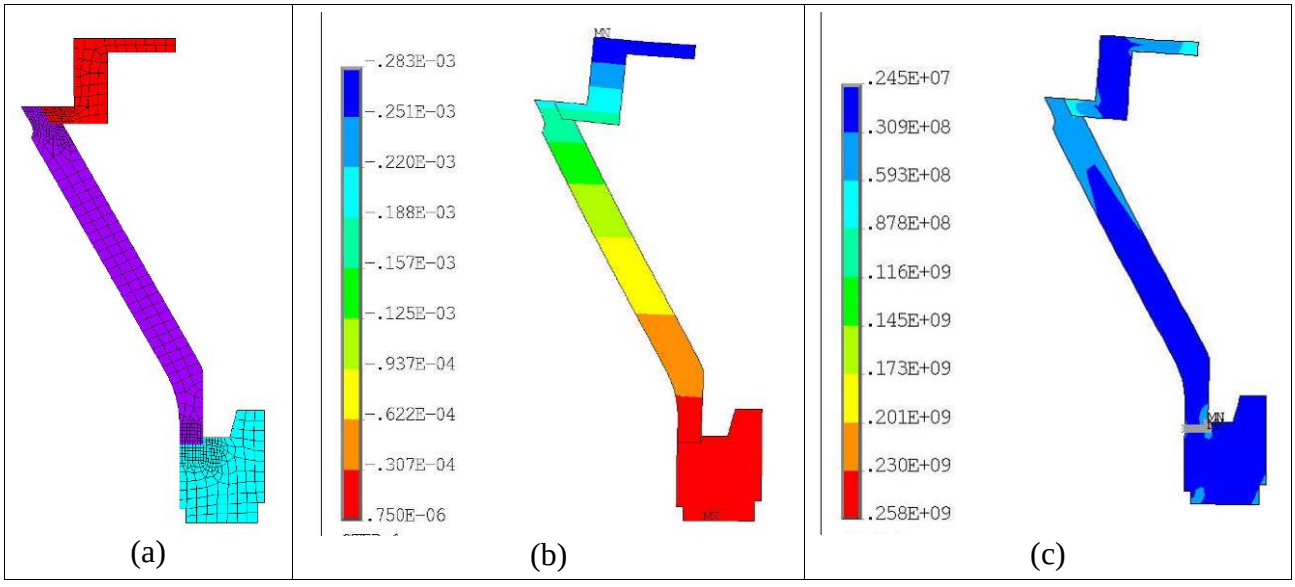

Figure 13: end dish coupler side: (a) FE mesh; (b) displacements and (c) stress for a force of 8667 N.

* This value has been obtained from experimental data available in literature and concerning the Nb RRR heat treated at 800 °C (Myneni et al.)

Evaluation of the end group stresses in working conditions (2.3.2)

Figure 13c shows an high stress concentration at the interface between the end dish and the Nb ring. This is due to the difference in the Young modulus of the two involved materials and to the fact that the materials have been considered as indefinitely elastic. Nevertheless the maximum stresses in the end dish (258 MPa) and in the adapting ring (88 MPa) are well below the yield limit of the material (see figure 14). The linear elastic analysis shows in the NbRRR a high stress concentration at the interface area: the maximum value is equal to 102 MPa (figure 15a). A further analysis, performed taking into account the material non-linearities, allows the estimation of the real maximum stress and the zone with plastic strains (figure 15b, maximum stress 51.5 MPa).

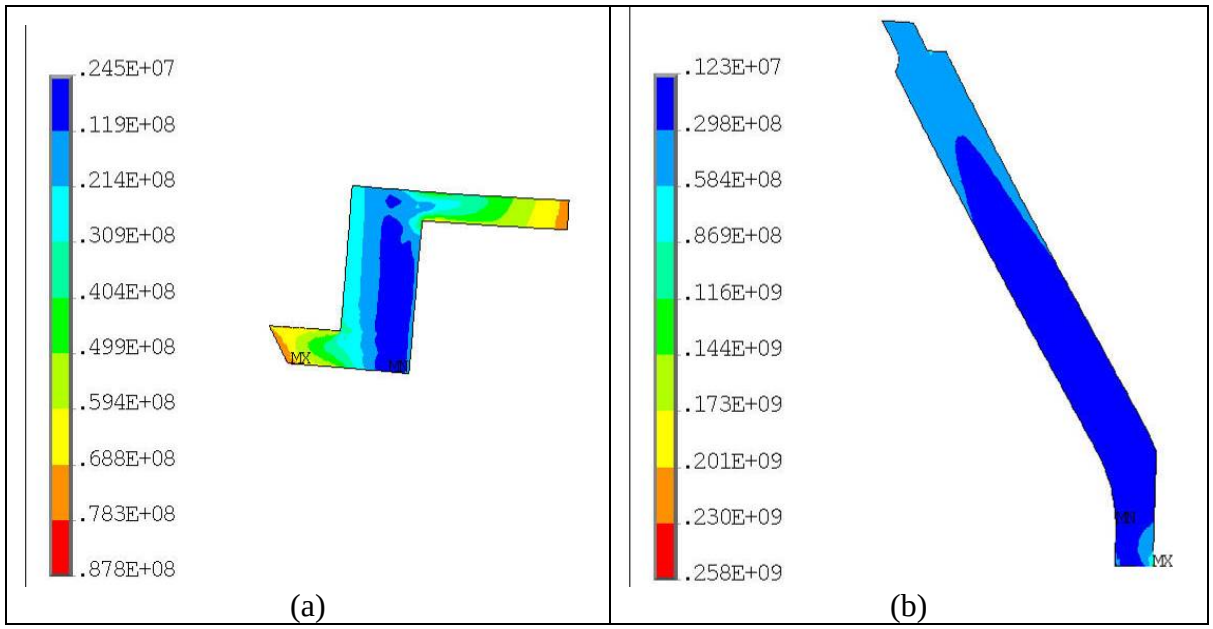

Figure 14: von Mises stresses in the adapting ring (a) and in the end dish (b).

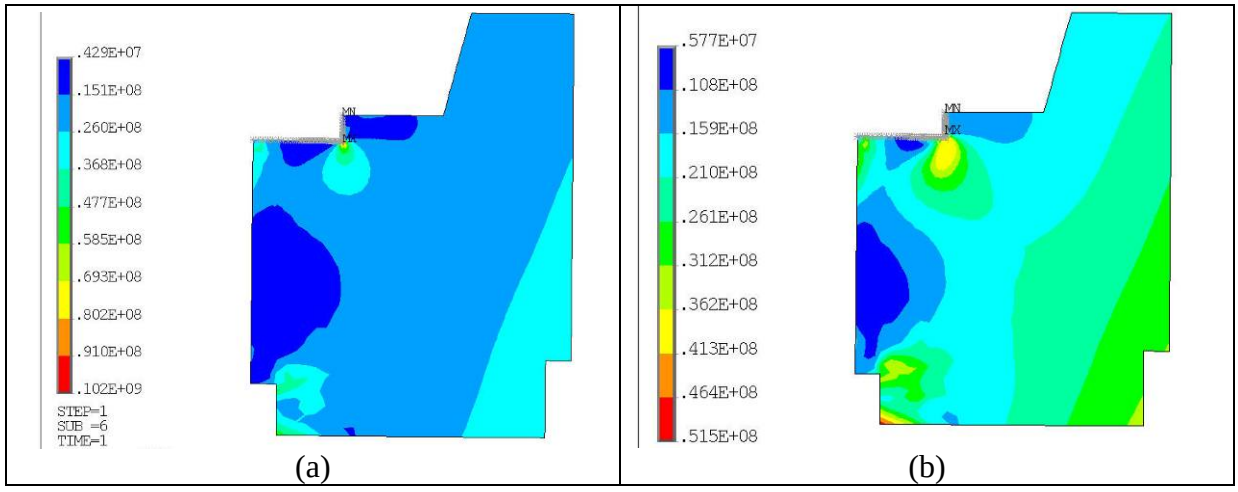

Figure 15: von Mises stresses in the Nb ring: (a) indefinitely elastic material, (b) bilinear elasto plastic material.

These results are considered as acceptable if we note that:

- the yield limit of 40 MPa is conservative, because it has been obtained at room temperature, while the yield stress at cryogenic temperature is higher;
- the area that exhibit plastic deformations is limited;
- these deformations do not affect the end group stiffness (30.4 vs. 30.6 kN/mm).

Evaluation of the end group stresses in acceptance test conditions (2.3.2)

The maximum compression load on the cavity happens during the acceptance pressure tests, where the helium tank and the end dishes are subjected to an internal pressure of 5.8 bar and the tuner withdrawn a traction of 14000 N. These forces have been applied to the FE model and the results are reported in figure 16 and figure 17.

The maximum stresses in the titanium adapting ring (83.4 MPa) and in the NbTi end dish (45.6 MPa) are well below their yield limits. The Nb ring exhibits a small yielded area in correspondence to the weld interface to the cavity, but this does not affect the safety of the structure.

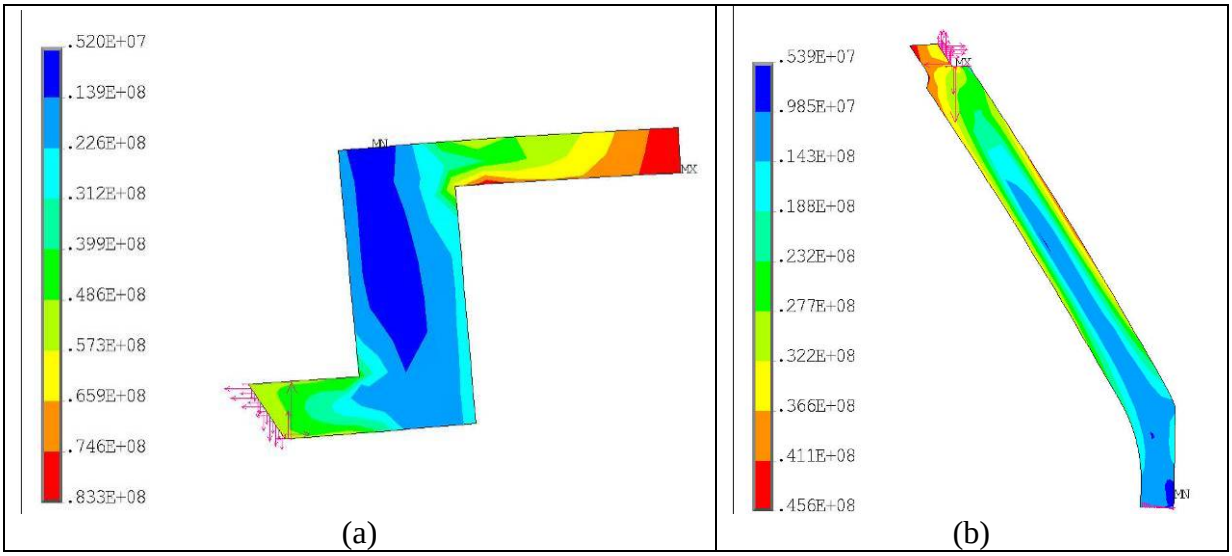

Figure 16: von Mises stresses in the adapting ring (a) and in the end dish (b)

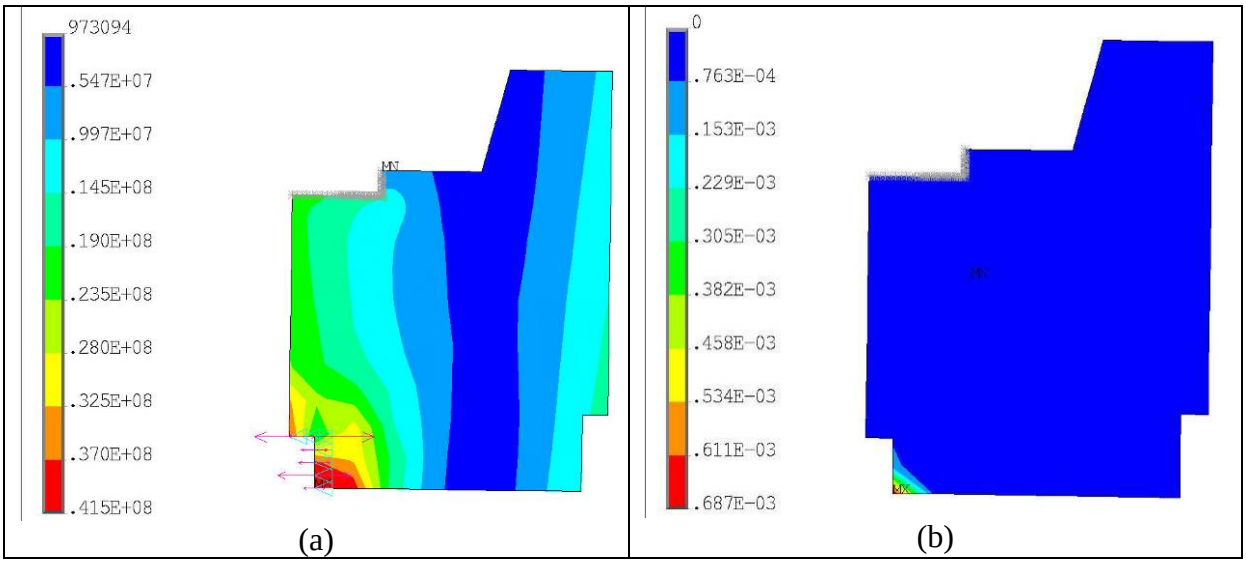

Figure 17: von Mises stresses in the Nb ring (a) and plastic deformations (b).

Second solution (internal number 2.5.1)

Geometry of the modified parts (2.5.1)

The proposed 2.5.1 end groups represent, in our opinion, one of the simplest possible configuration as the one adopted for the 3.9 GHz XFEL cavity [3]. The reference surfaces are machined both on the end dish and on the Nb ring, in a different position with respect to the TTF/XFEL solution. This arrangement is not fully compatible with the existing tuning device, support systems and other tools that have to be connected with the actual Nb ring. Furthermore, this solution is only suitable for the coaxial tuner, and not compatible with the lateral one.
The technical drawings of the main parts involved in this proposal are reported in appendix B.

End group preparation (2.5.1)

The foreseen welding steps are reported in figure 18. As for the solution 2.3.2, only two loadings in the EB welding machine are required: in the first one the end dish is welded to the NbRRR ring, while in the second one the end cell and the pipe are assembled to the ring.

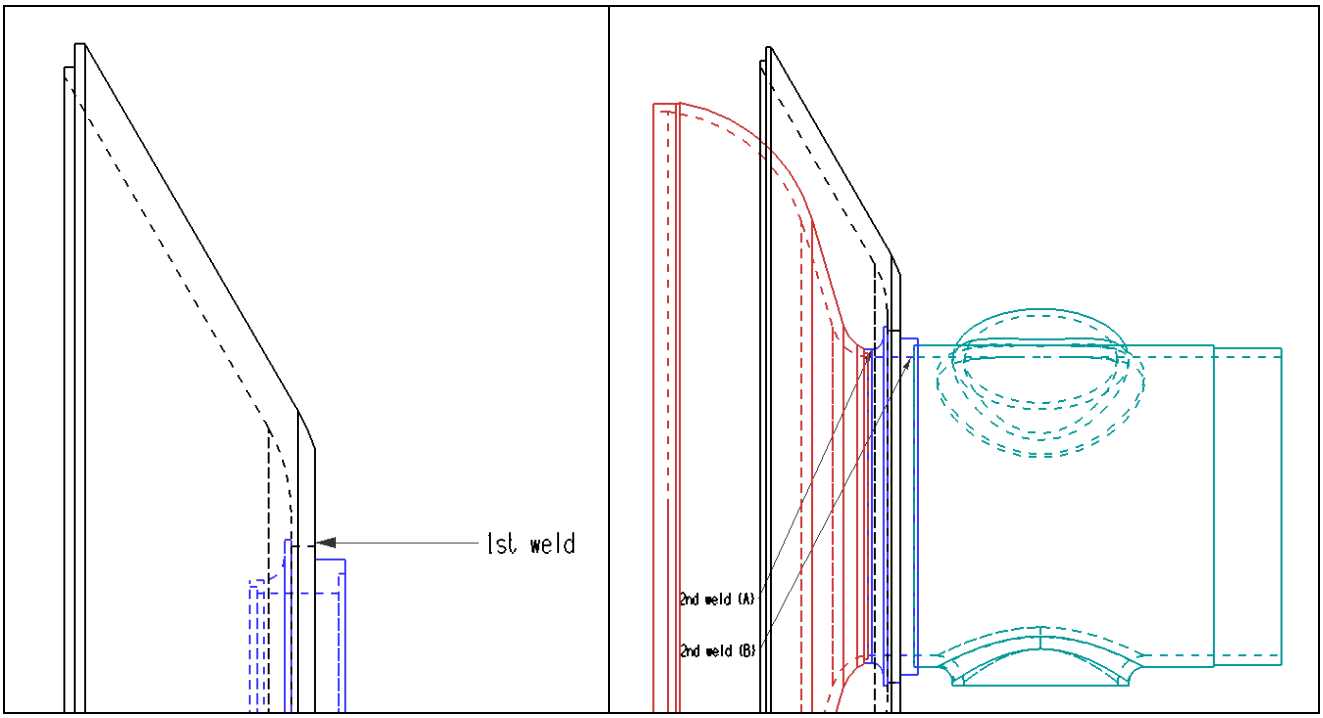

Figure 18: welding sequence.

Helium tank and its interface to the cavity (2.5.1)

The helium tank here proposed has been designed to be used with the coaxial tuner. For this reason it is separated in two parts by means of a bellow, and the connection to the end dishes is slightly different from respect to the proposal 2.3.2.
A picture of the helium tank is reported in Figure 19. The central bellow and the different shape of the lateral faces are evident. A detail of the connection to the end dishes and of the part that should accord the cavity and the helium tank length are reported in Figure 20 and in Figure 21.

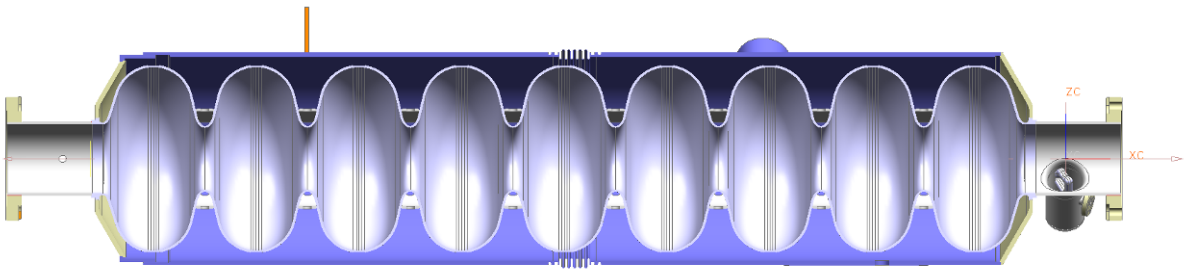

Figure 19: longitudinal section of the 2.5.1 proposal integrated in the helium tank.

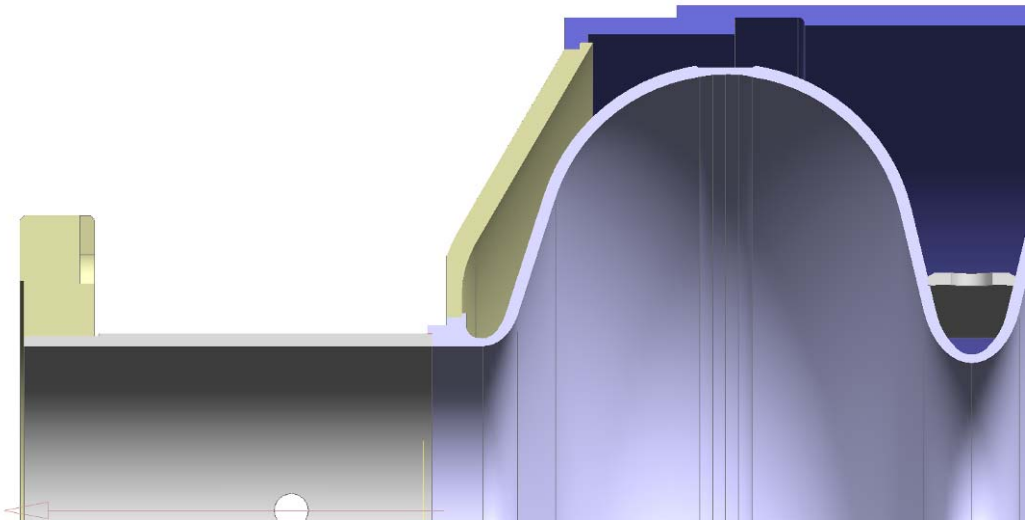

Figure 20: end dish connection to the He tank at the side without the main coupler. It is visible the adapting ring.

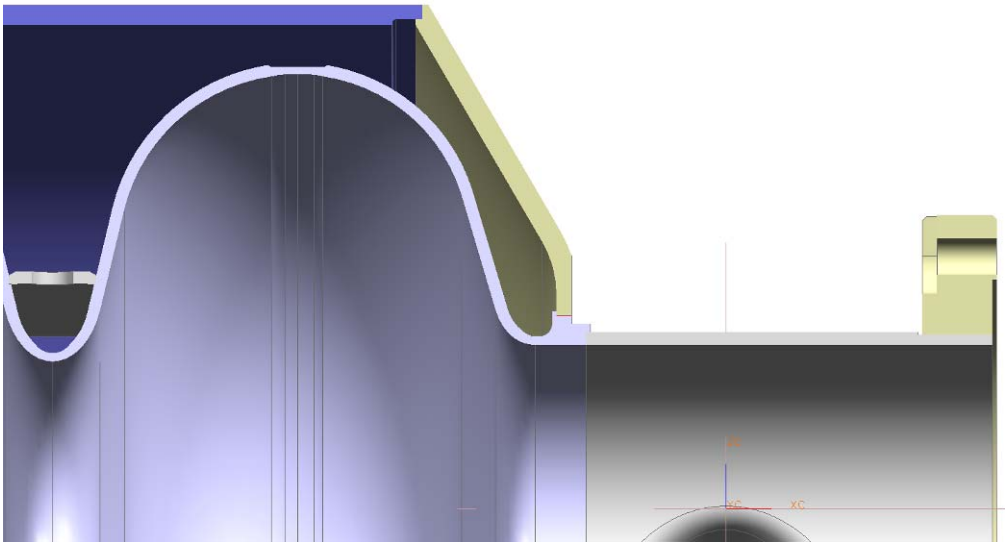

Figure 21: end dish connection to the HT at the main coupler side.

Mechanical analysis of the end group coupler side (2.5.1)

For the same reason of the first proposal, the analyses of the end group has been limited to the coupler side. The deformations and stresses of the end dish, in different load conditions, are evaluated by means of a FE linear analysis. The material properties at room temperature are the same of the solution 2.3.2, while the axisymmetric mesh is reported in figure 22 (a). The end tube has been modelled for 50 mm length to take into account its contribution to the stiffness (not shown in figure 22).

Evaluation of the end group stiffness (2.5.1)

In order to evaluate the axial stiffness of this solution, an analysis has been performed applying a force of 8667 N at the top of the end dish (as for the proposal before presented). In this analysis the materials have been considered indefinitely elastic and the maximum displacement obtained is equal to 0.266 mm. The axial stiffness of the end dish at the coupler side is equal to 32.6 kN/mm (8667 N/0.266 mm). The plot of the displacements and of the von Mises stresses are reported in Figure 22 (b) and (c).

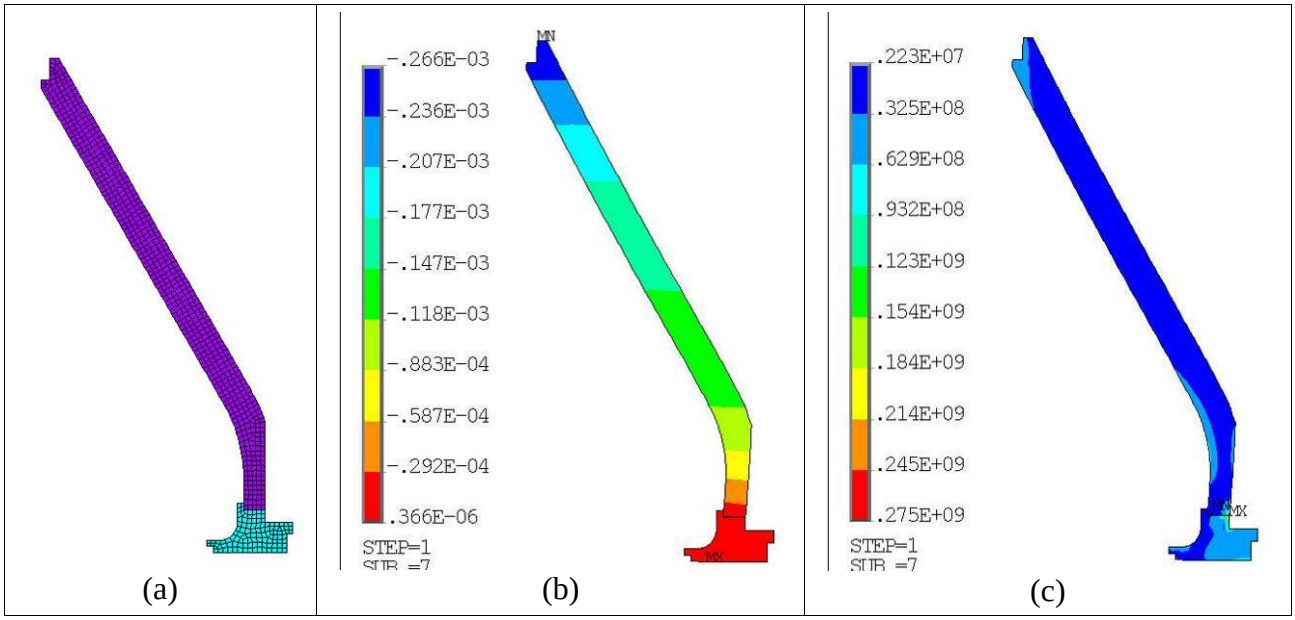

Figure 22: end dish coupler side: (a) FE mesh; (b) displacements and (c) stress for a force of 8667 N.

Evaluation of the end group stresses in working conditions (2.5.1)

Figure 22 shows an high stress concentration at the interface between the end dish and the Nb ring. This is due to the difference in the Young modulus of the two involved materials and to the fact that the materials have been considered as indefinitely elastic. Nevertheless the maximum stress in the end dish (153 MPa) is well below the yield limit of the material (see figure 23), while a not negligible area of the NbRRR ring exhibits plastic deformations (figure 24, maximum stress 52.8 MPa considering the yielding of the material).

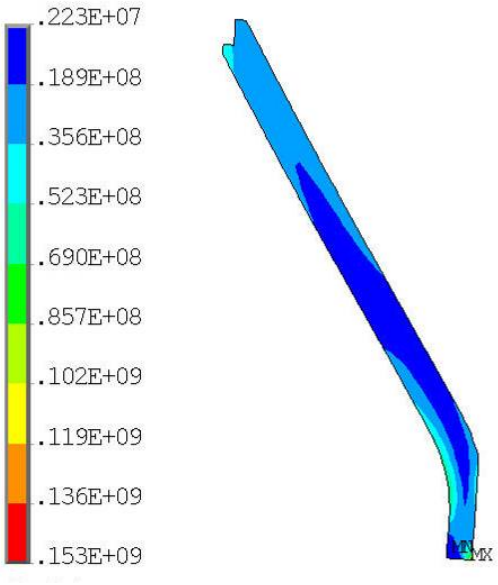

Figure 23: von Mises stresses in the end dish.

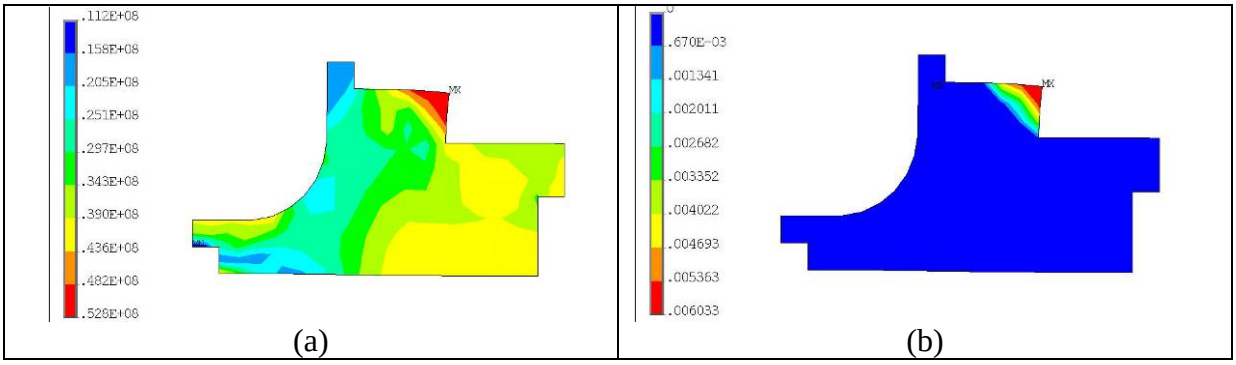

Figure 24: (a) von Mises stresses in the Nb ring and (b) plastic deformations.

Despite of these high stresses occurs at cryogenic temperature and at the higher bound of the tuning range, the results are unacceptable for the safety of the structure (plastic strains spread on about half of the welding area). Furthermore, the computed displacement considering the plastic deformations is equal to 0.3 mm, and the stiffness drop to 8667/0.3 = 28.9 kN, 12% less than neglecting the plastic strains.

Evaluation of the end group stresses in acceptance test conditions (2.5.1)

The maximum load on the cavity happens during the acceptance tests, where the helium tank and the end dishes are subjected to an external pressure of 5.8 bar and the tuner is subjected to a compression of 14000 N. These forces have been applied to the FE model and the results are reported in Figure 25 and figure 26.
The maximum stress in the end dish (79.8 MPa) is well below the yield limit. The Nb ring exhibits plastic deformations in correspondence to the welds, with an extension not acceptable from the safety point of view.

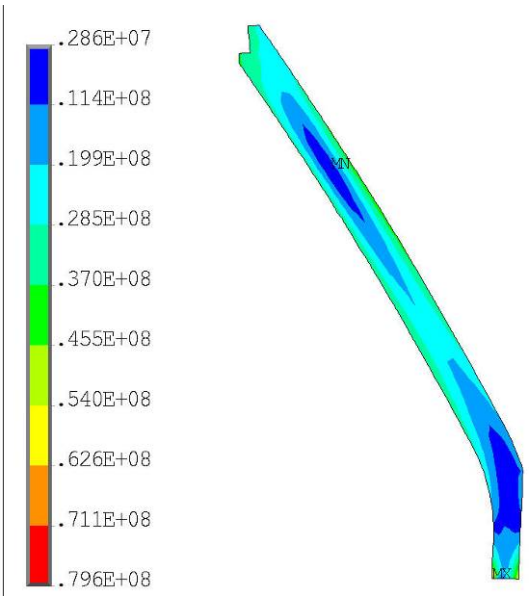

Figure 25: von Mises stresses in the end dish.

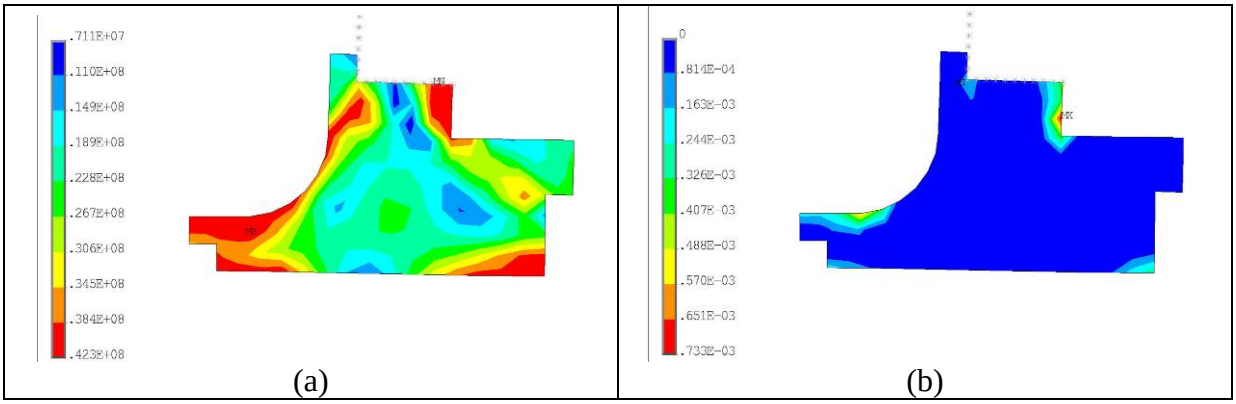

Figure 26: von Mises stresses in the Nb ring (a) and plastic deformations (b).

Conclusions

Our work relative to the cavity optimization leads to positive results. First of all we built a prototype, based on the usual cavity to helium tank interface, that allowed us to perform the tests at cold temperature with the coaxial blade tuner. This was useful to validate our numerical model of the whole assembly.
On the basis of the experimental results, we analyzed several new configurations with the final goal of getting a simple and cheaper end group solution, with a higher stiffness.
At the end, two different configurations have been highlighted and deeply investigated.

Solution	Combined stiffness	Pro	Cons
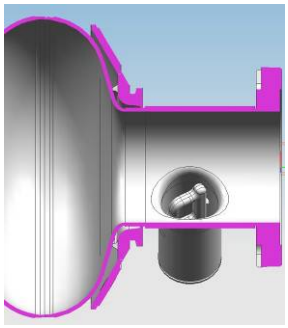 TTF/XFEL	k_w = 14 kN/mm k^T_w = 32.2 kN/mm k^C_w = 24.8 kN/mm	• Existing tools for tuning and supporting • Chemical treatment of surfaces to be weld can be done without interfering with the NbTi end disc • Proved geometry	• ring geometry very complicated • Low axial stiffness • High number of welds
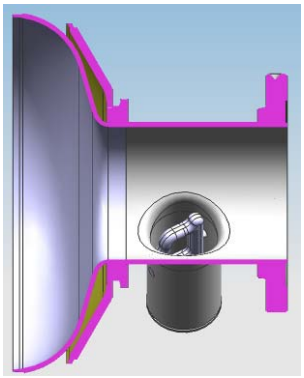 2.3.2	k_w = 13.5 kN/mm k^T_w = 30.6 kN/mm k^C_w = 24.2 kN/mm	• Existing tools for tuning and supporting • The weld sequence is simpler due to the absence of the end cell reinforcing tooth • Geometry of the ring simplified • Reduced number of EB welds • Full compatibility with XFEL helium tanks • Proved integration procedure into the helium tank	• The Nb ring must be fabricated in RRR • Low axial stiffness • The end disc must be protected before the chemical treatment required for the welds • 6% more of LFD • Integration into the helium tank require an adapting ring and the lateral bellow.
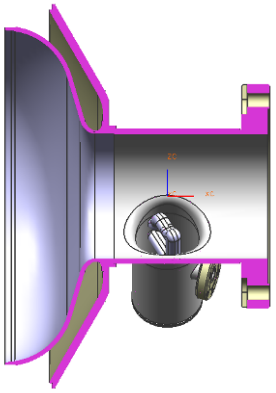 2.5.1	k_w = 16.2 kN/mm k^T_w = 32.6 kN/mm k^C_w = 32.2 kN/mm	• Small and simple ring • The weld sequence is simpler due to the absence of the end cell reinforcing tooth • Reduced number of EB welds • High axial stiffness • Two reference planes as in 3.9 GHz cavity • Reduced number of welds for the integration into the helium tank.	• Incompatibility with the existing tools for tuning and supporting • The end disc must be protected before the chemical treatment required for the welds • The Saclay tuner can not be installed • 6% more of LFD • Critical for plastic strains

Table 7: different configurations examined

To check finally our work we decided to produce two simplified end groups of the type 2.3.2, that are now under construction (figure 27 and figure 28, see drawings in appendix C). The goals of this final step are:

- to check the simplified welding procedure on the new end groups;
- to evaluate the welding shrinkages;
- to evaluate the deformation of the last end cells after the weld procedure, that we expect to be lower than the current solution because of the lack of the end cells stiffening welding;
- to measure the axial stiffness of the new end group with an arrangement similar to that reported in figure 29 and figure 30.

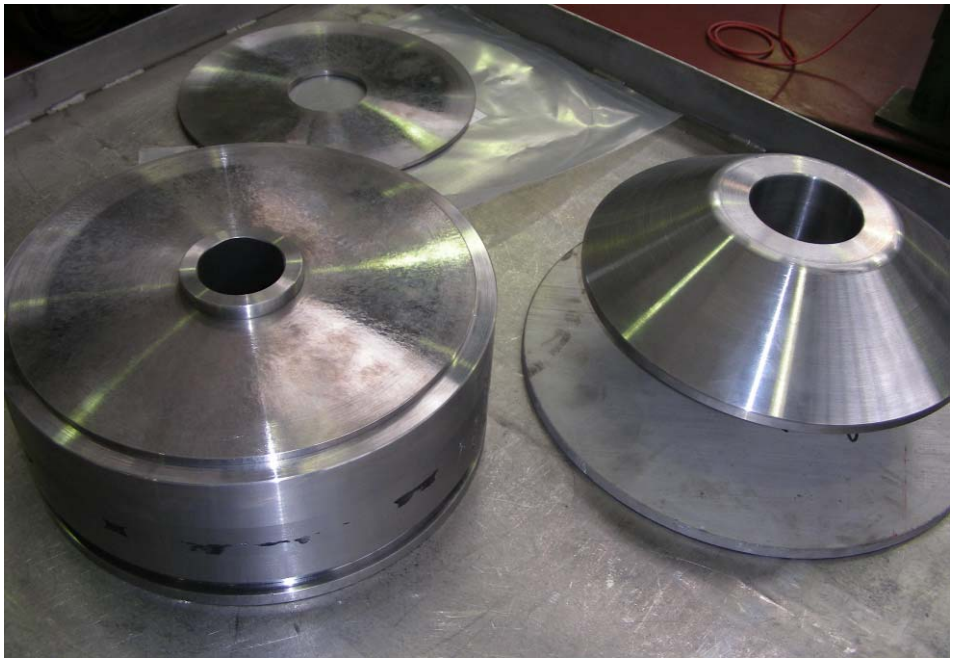

Figure 27: tool for NbTi end dish deep drawing

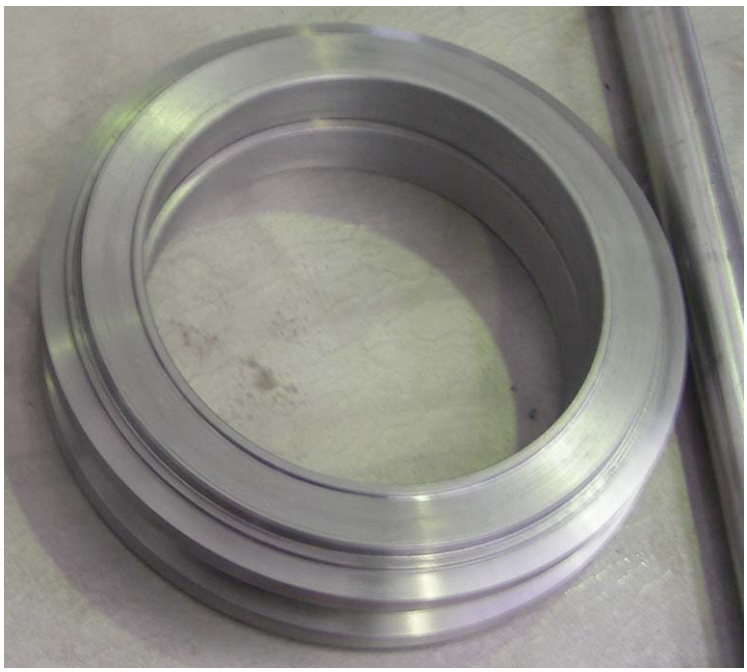

Figure 28: NbRRR connecting rings ready for e beam welding

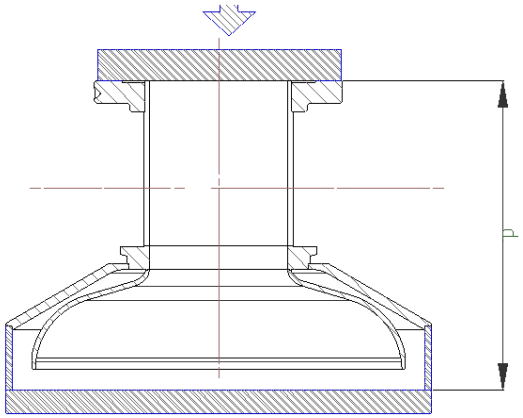

Figure 29: scheme of the compression test for the characterization of the end dish stiffness

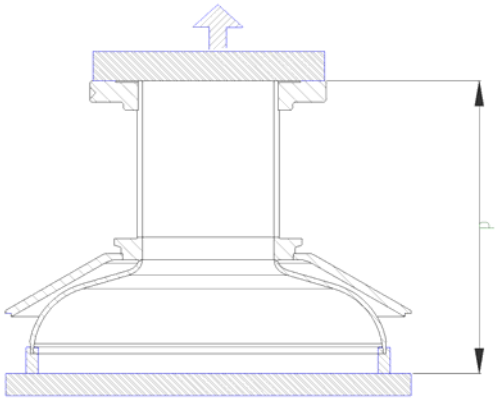

Figure 30: scheme of the traction test for the characterization of the half cell stiffness

Reference

[1] ILC Design report – Volume 3 – The Accelerator (http://ilcdoc.linearcollider.org/getfile.py?docid=182&name=ILC_RDR_Volume_3-Accelerator&format=pdf)

[2] C. Pagani, A. Bosotti, P. Michelato, N. Panzeri, R. Paparella, and P. Pierini, "The fast piezo-blade tuner for SCRF resonators," in *Proc. Proceedings of 12th International Workshop on RF Superconductivity (SRF 2005)*, July 2005.

[3] P. Pierini et al., “Third harmonic superconducting cavity prototypes for the XFEL”, THP019 - proc. LINAC2008,.Victoria, British Columbia, Canada, 2008.

[4] A. Bosotti et al., “The Coaxial Blade Tuner – Final Report and Evaluation of Operation”, CARE-Report-2008-018-SRF, 2008.

Appendix A : drawings end group v. 2.3.2

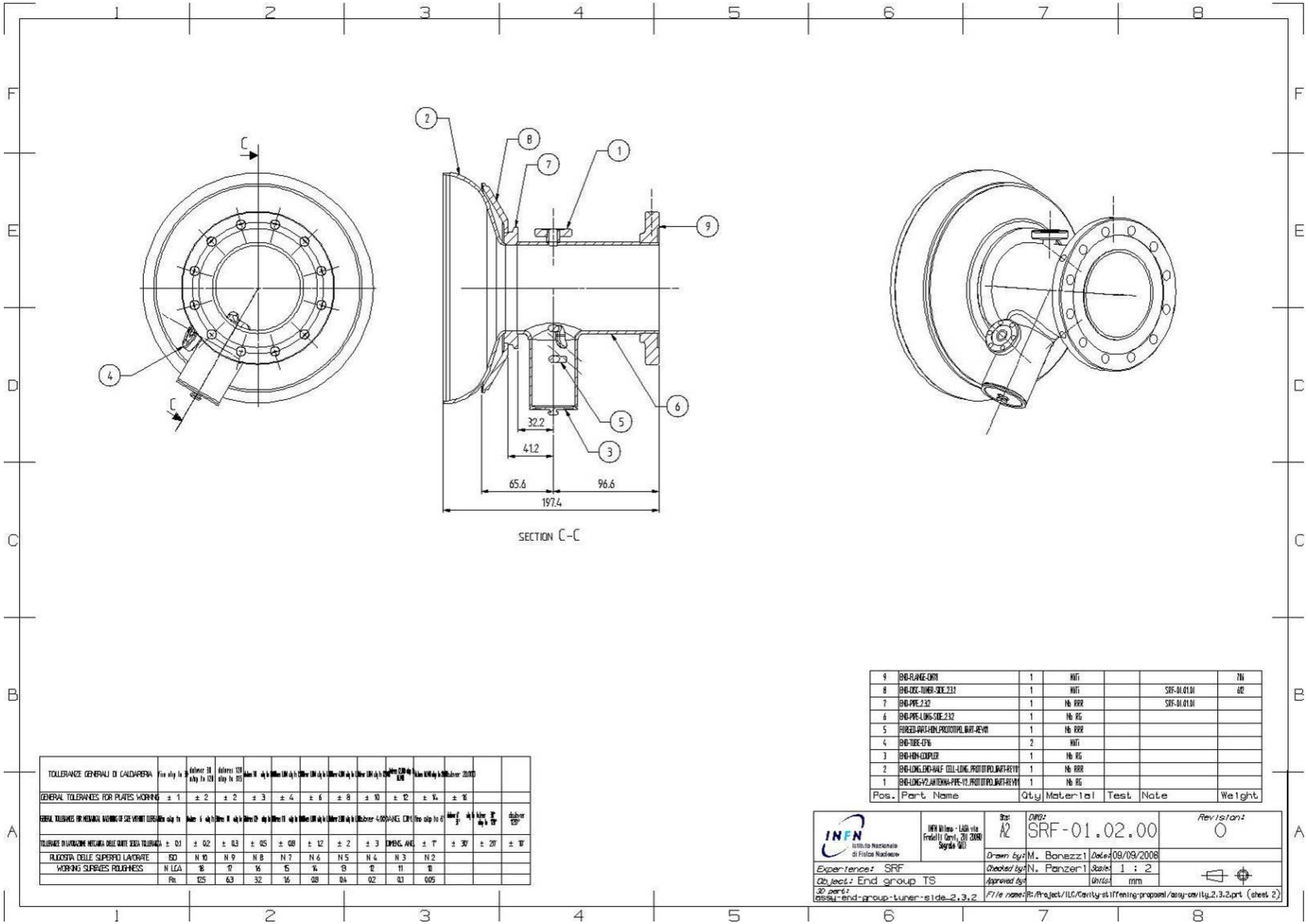

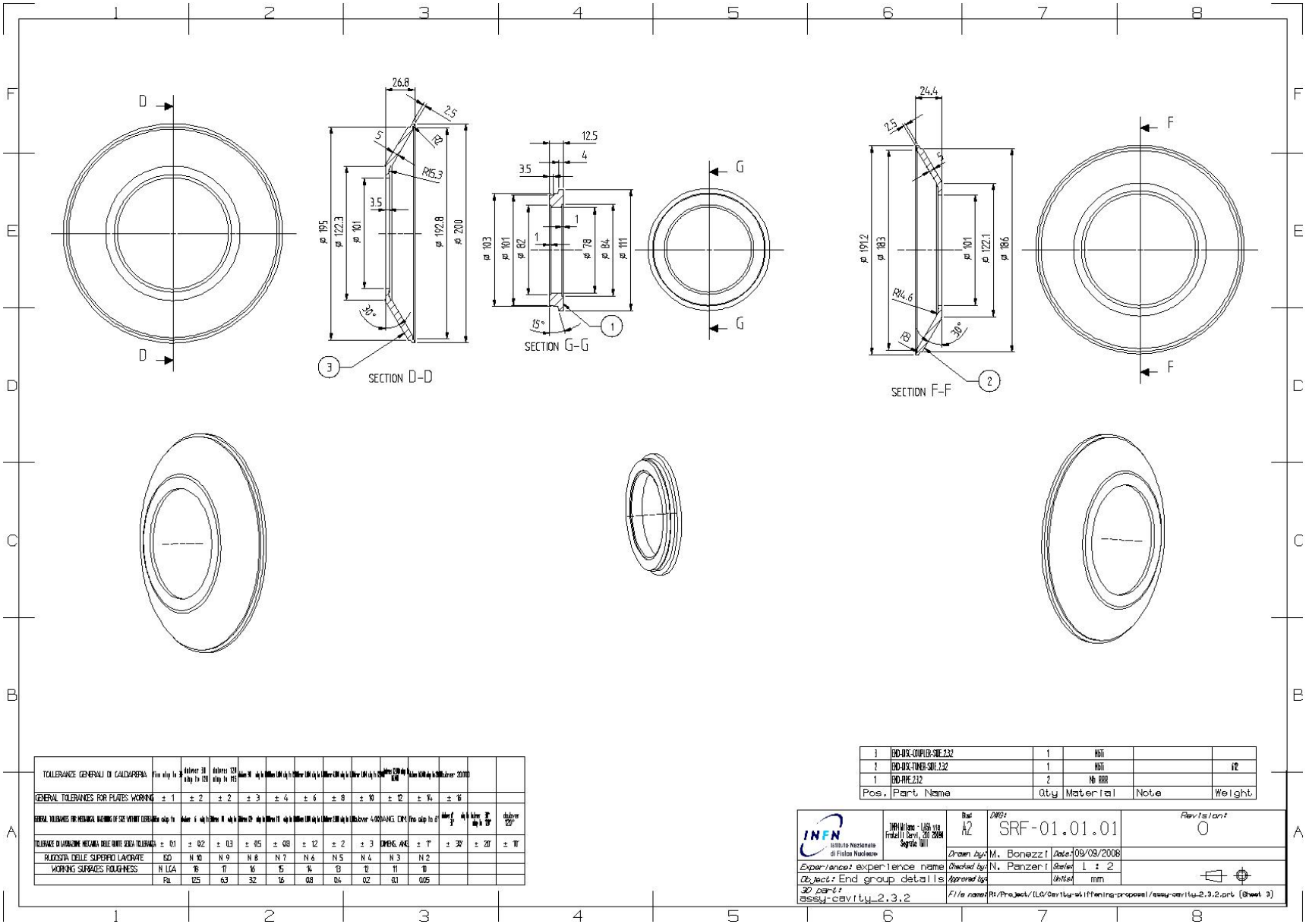

3	END-DISC-COUPLER-SIDE.2.3.2	1	NbTi			
2	END-DISC-TUNER-SIDE.1.3.2	1	NbTi			ø2
1	END-PIPE.2.1.2	2	Nb RRR			
Pos.	Part Name	Qty	Material	Note	Weight	

INFN Istituto Nazionale di Fisica Nucleare	INFN Milano - LASA via Fratelli Cervi, 201 20054 Segrate (MI)	Sheet: A2	DWG#: SRF-01.01.01	Revision: 0
		Drawn by: M. Bonezzi	Date: 09/09/2008	
Experiment: experience name		Checked by: N. Panzeri	Scale: 1 : 2	
Object: End group details		Approved by:	Units: mm	
3D part: assy-cavity_2.3.2		File name: R:/Project/ILC/Cavity-stiffening-proposal/assy-cavity_2.3.2.prt (Sheet 3)		

Appendix B : drawings end group v. 2.5.1

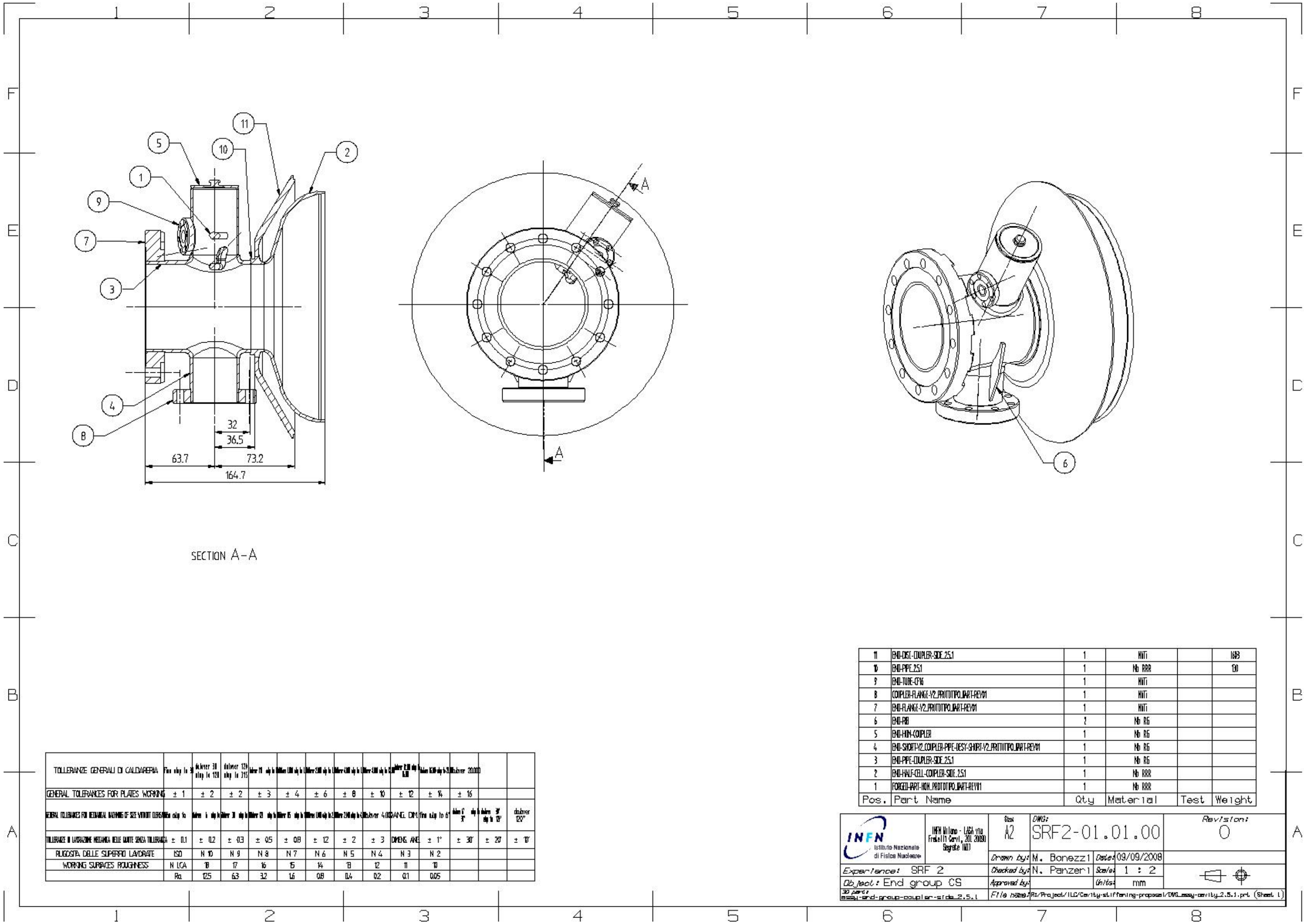

 P:\0 - 0 - 0 SESTOPROGRAMMAQUADRO\SRF\2_2_5\cavity-report-final-version_mic_comp.doc

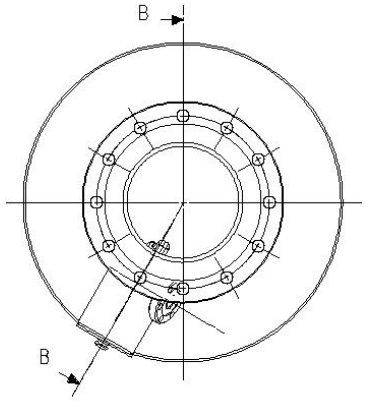

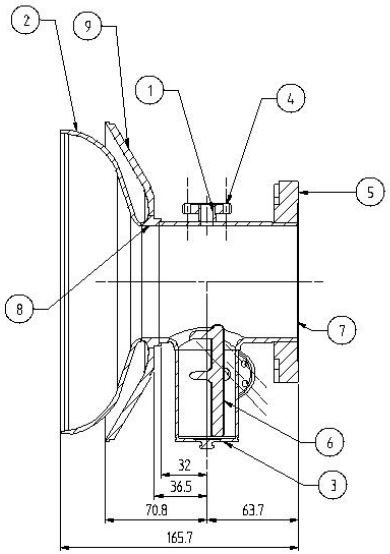

SECTION B-B

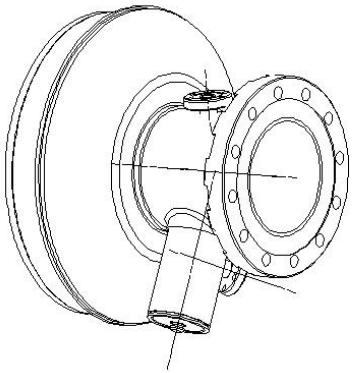

9	END-BSC-PIEZO-SIDE_2.5.0	1	NbTi		BCP
8	END-PIPE_2.5.1	1	Nb RRR		BCP
7	END-PIPE-LONG-SIDE_2.5.1	1	Nb RG		
6	FORGED-WAT-HOM_PROTOTIPO_PART-REV01	1	Nb RRR		
5	END-FLANGE-V2_PROTOTIPO_PART-REV01	1	NbTi		
4	END-TUBE-CF16	2	NbTi		
3	END-HOM-COUPLER	1	Nb RG		
2	END-VALVE-FULL-LONG-SIDE_2.5.1	1	Nb RRR		
1	END-LONG-V2_ANTENNA-PIPE-V2_PROTOTIPO_PART-REV01	1	Nb RG		
Pos.	Part Name	Qty	Material	Note	Weight

TOLLERANZE GENERALI DI CALDARERIA	fino a/up to 30	oltre/over 30 fino a/up to 120	oltre/over 120 fino a/up to 315	oltre/over 315 fino a/up to 1000	oltre/over 1000 fino a/up to 2000	oltre/over 2000 fino a/up to 3150	oltre/over 3150 fino a/up to 4000	oltre/over 4000 fino a/up to 6300	oltre/over 6300 fino a/up to 10000	oltre/over 10000 fino a/up to 16000	oltre/over 16000 fino a/up to 25000	oltre/over 25000	
GENERAL TOLERANCES FOR PLATES WORKING	± 1	± 2	± 2	± 3	± 4	± 6	± 8	± 10	± 12	± 14	± 16		
GENERAL TOLERANCES FOR MECHANICAL MACHINING IF SEE INTERNAL TOLERANCES	fino a/up to 1	oltre/over 1 fino a/up to 3	oltre/over 3 fino a/up to 6	oltre/over 6 fino a/up to 30	oltre/over 30 fino a/up to 120	oltre/over 120 fino a/up to 400	oltre/over 400 fino a/up to 1000	oltre/over 1000 fino a/up to 2000	oltre/over 2000 ANGOLARE/ANG. DIM.	fino a/up to 10	oltre/over 10 fino a/up to 50	oltre/over 50 fino a/up to 120	oltre/over 120°
TOLLERANZE DI LAVORAZIONE MECCANICA DELLE QUOTE SENZA TOLLERANZA	± 0.1	± 0.2	± 0.3	± 0.5	± 0.8	± 1.2	± 2	± 3	DIVERS. ANG.	± 1°	± 30'	± 20'	± 10'
RUGOSITÀ DELLE SUPERFICI LAVORATE	ISO	N 10	N 9	N 8	N 7	N 6	N 5	N 4	N 3	N 2			
WORKING SURFACES ROUGHNESS	N UCA	18	17	16	15	14	13	12	11	10			
	Ra	12.5	6.3	3.2	1.6	0.8	0.4	0.2	0.1	0.05			

INFN Istituto Nazionale di Fisica Nucleare	INFN Milano - LASA via Fratelli Cervi, 201 20090 Segrate (MI)	Sheet: A2	DWG: SRF2-01.02.00	Revision: 0
		Drawn by: M. Bonezzi	Date: 09/09/2008	
Experience: SRF 2		Checked by: N. Panzeri	Scale: 1 : 2	
Object: end group PS		Approved by:	Units: mm	
3D part: assy-end-grp-v2-piezo-side_2.5.1		File name: R:/Project/TLC/Cavity-stiffening-proposal/DWG/assy-cav1y_2.5.1.prt (Sheet 2)		

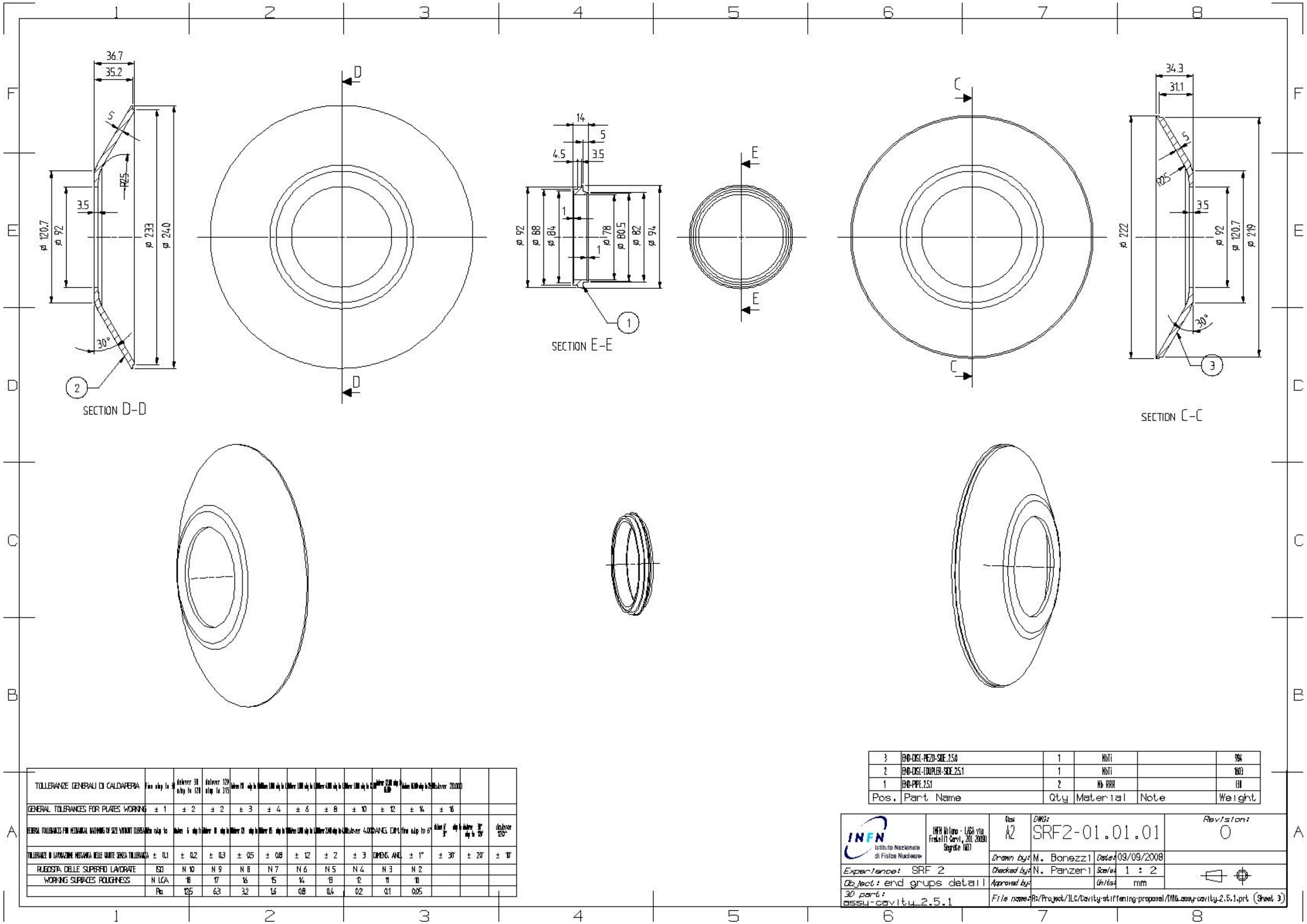

SECTION D-D
SECTION E-E
SECTION C-C
TOLLERANZE GENERALI DI CALDARERIA
GENERAL TOLERANCES FOR PLATES WORKING
RUGOSITA DELLE SUPERFICI LAVORATE
WORKING SURFACES ROUGHNESS
3 END-DISC-PIEZO-SIDE.2.5.0 1 NbTi 984
2 END-DISC-COUPLER-SIDE.2.5.1 1 NbTi 1603
1 END-PIPE.2.5.1 2 Nb RRR 1311
Pos. Part Name Qty Material Note Weight
INFN Istituto Nazionale di Fisica Nucleare
INFN Milano - LASA via Fratelli Cervi, 201 20090 Segrate (MI)
Size A2
DWG: SRF2-01.01.01
Revision: 0
Drawn by: M. Bonezzi Date: 09/09/2008
Checked by: N. Panzeri Scale: 1 : 2
Approved by: Units: mm
Experience: SRF 2
Object: end grups detail
3D part: assy-cavity_2.5.1
File name: R:/Project/ILC/Cavity-stiffening-proposal/DWG_assy-cavity_2.5.1.prt (Sheet 3)

Appendix C : drawings end group v. 2.3.2 to be built

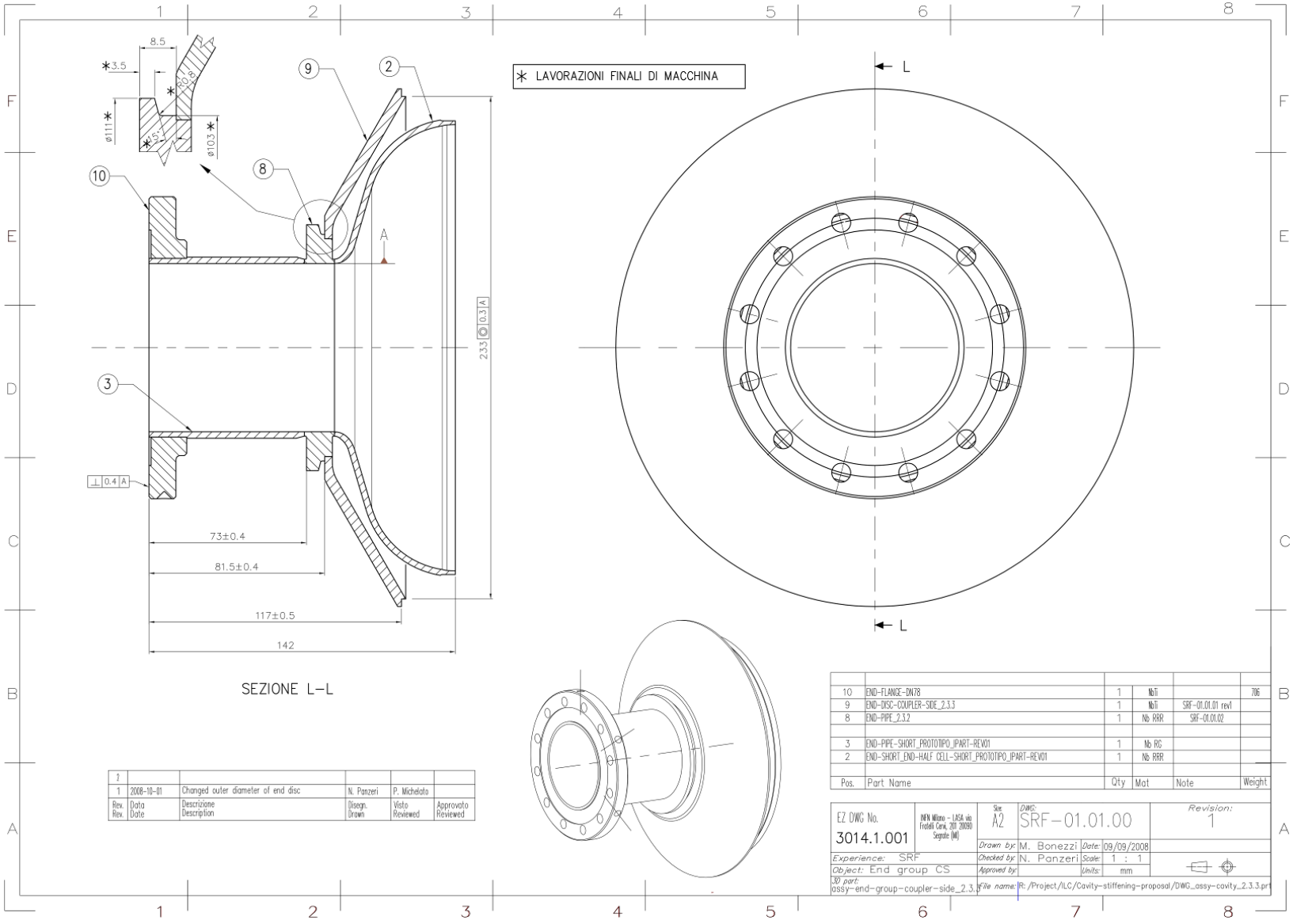

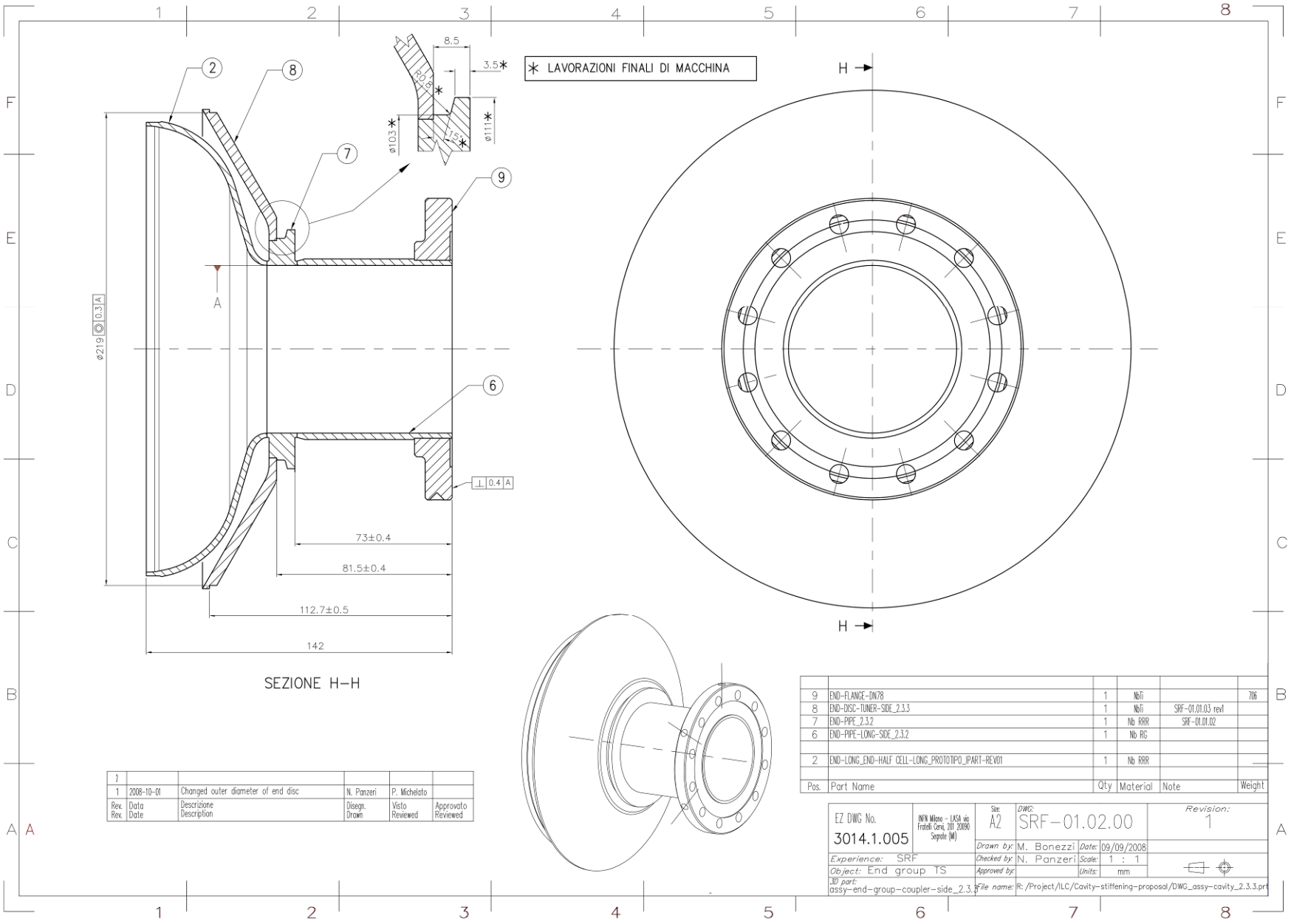

Rev.	Data Date	Descrizione Description	Disegn. Drawn	Visto Reviewed	Approvato Reviewed
2					
1	2008-10-01	Changed outer diameter of end disc	N. Panzeri	P. Michelato	

Pos.	Part Name	Qty	Material	Note	Weight
9	END-FLANGE-DN78	1	NbTi		706
8	END-DISC-TUNER-SIDE_2.3.3	1	NbTi	SRF-01.01.03 rev1	
7	END-PIPE_2.3.2	1	Nb RRR	SRF-01.01.02	
6	END-PIPE-LONG-SIDE_2.3.2	1	Nb RG		
2	END-LONG_END-HALF CELL-LONG_PROTOTIPO_IPART-REV01	1	Nb RRR		

EZ DWG No. 3014.1.005
INFN Milano – LASA via Fratelli Cervi, 201 20090 Segrate (MI)
Size: A2
DWG: SRF-01.02.00
Revision: 1
Drawn by: M. Bonezzi Date: 09/09/2008
Checked by: N. Panzeri Scale: 1 : 1
Approved by: Units: mm
Experience: SRF
Object: End group TS
3D part: assy-end-group-coupler-side_2.3.3
File name: R: /Project/ILC/Cavity-stiffening-proposal/DWG_assy-cavity_2.3.3.prt